

# **Oceanographic conditions off northern Chile during the 1996 La Niña and 1997-1998 El Niño: Part 1: Hydrographic conditions**

Jose Luis Blanco

Instituto de Fomento Pesquero, Valparaíso, Chile

Mary-Elena Carr

Jet Propulsion Laboratory, California Institute of Technology, Pasadena, CA

Andrew C. Thomas

School of Marine Sciences, University of Maine, Orono, ME

P. Ted Strub

College of Oceanic and Atmospheric Sciences, Oregon State University, Corvallis, OR

Corresponding author address: M.-E. Carr, Jet Propulsion Laboratory MS 300-323, California Institute of Technology, 4800 Oak Grove Dr., Pasadena, CA 91009  
([mec@pacific.jpl.nasa.gov](mailto:mec@pacific.jpl.nasa.gov))

Short title: HYDROGRAPHIC CONDITIONS OFF NORTHERN CHILE 1996-1998

## Abstract.

The evolution of oceanographic conditions in the upwelling region off northern Chile ( $18^{\circ}$ - $24^{\circ}$ S) between 1996 and 1998 (including the 1997-1998 El Niño) is presented using hydrographic measurements acquired on quarterly cruises of the Chilean Fisheries Institute, sea-surface temperature (SST), sea level, and wind speeds from Arica ( $18.5^{\circ}$ S), Iquique ( $20.5^{\circ}$ S), and Antofagasta ( $23.5^{\circ}$ S), and a time series of vertical temperature profiles off Iquique. Spatial patterns of sea surface temperature and salinity from May 1996 to March 1997 followed a normal seasonal progression though conditions were anomalously cool and fresh. Starting in March 1997, positive anomalies in sea level and sea surface temperature propagated along the South American coast to  $37^{\circ}$ S. Maximum sea level anomalies occurred in two peaks in May-July 1997 and October 1997-February 1998, separated by a relaxation period. Maximum anomalies ( $2^{\circ}$ C and 0.1 practical salinity units or psu) extended to 400 m in December 1997 within 50 km of the coast. March 1998 presented the largest surface anomalies ( $>4^{\circ}$ C and 0.6 psu). Strong poleward flow ( $20$ - $35\text{ cm s}^{-1}$ ) occurred to 400 m or deeper during both sea level maxima and weaker ( $10\text{ cm s}^{-1}$ ) equatorward flow followed each peak. By May 1998, SST had returned to the climatological mean and flow was equatorward next to the coast. However, offshore salinity remained anomalously high due to a tongue of SubTropical Water extending southeast along the Peruvian coast. Conditions off northern Chile returned to normal between August and December 1998. The timing of the anomalies suggest a connection to equatorial waves. The progression of the 1997-1998 El Niño was very similar to that of 1982-1983 though with different timing with respect to seasons.

# 1. Introduction and Background

## Introduction

The coastal ocean off northern Chile between 18° and 24°S (Figure 1) is characterized by wind-driven coastal upwelling, which leads to elevated biological productivity. The region is embedded in the Peru-Chile Current System. Water flowing eastward in the South Pacific Current (West Wind Drift) reaches Chile between 35° and 45°S and splits into the southward flowing Cape Horn Current and the northward flowing Peru-Chile Current, also known as the Humboldt or Peru Current. Although the circulation in this region is often portrayed in schematics as simply equatorward, it is a complex system (Strub *et al.*, 1998) comprising nearshore and offshore equatorward branches, a poleward undercurrent next to the coast, and one or more surface poleward countercurrents that may be connected to the undercurrent.

Monthly averaged winds off northern Chile blow from the south or southwest year-round with speeds of 3-6 m s<sup>-1</sup>. The maximum is in austral summer, unlike off the Peruvian coast where the maximum wind occurs in fall- winter. Wind speeds are lower and the seasonal cycle weaker in the northeast corner, where the coastline changes from a zonal to a more meridional orientation. The equatorward winds drive coastal upwelling, which lifts the thermocline/nutricline, supplying nutrients to the surface and enabling phytoplankton growth. This translates into a strong fishery for small pelagic fish. Approximately two million metric tons (MMT) of anchovy and sardines are landed during normal years off northern Chile and make up one third of the total Chilean catch.

The seasonal variation in the hydrographic patterns in this region results from the solar cycle and shifts in transport of the major upper-ocean water masses. Long-term hydrographic measurements of the region (Blanco *et al.*, 2000) have been used to define the regional characteristics of these water masses. XX The warm ( $>18.5^{\circ}\text{C}$ ) and salty ( $>34.9$ ) Subtropical Water (STW), observed at the surface, has its source northwest of Peru. The cooler ( $\sim 12.5^{\circ}\text{C}$ ) and relatively salty (34.7-34.9) Equatorial Subsurface Water (ESSW) makes up the poleward undercurrent between 100-300 m depth near the continental slope. STW and ESSW are of equatorial/subtropical origin and their influence is maximum in the northern portion of the study area and decreases to the south. The cool ( $\sim 12^{\circ}$ ) and fresh ( $\sim 34.25$ ) Subantarctic Water (SAW) has a far southern source and is found below the STW offshore and above the ESSW closer to the coast. Below 500 m the influence of the cold ( $\sim 7^{\circ}$ ) and fresh ( $\sim 34.4$ ) Antarctic Intermediate Water (AIW) can be seen. SST and surface salinity present a strong cross-shelf gradient in spring and summer due to warming of offshore waters and upwelling of cool, fresher water (a combination of ESSW from the poleward undercurrent and SAW) near the coast. The meridional gradient results from the northern influence of warm, salty STW at the surface. In winter and fall, the surface fields are usually homogeneous with a weak north-south gradient. Blanco *et al.* (2000) describe the climatological seasonal cycles of wind forcing, water properties, and circulation between  $18^{\circ}$  and  $24^{\circ}\text{S}$ .

This region is subject to large interannual variability associated with the El Niño-Southern Oscillation (ENSO) ‘cycle’. Conditions that are typically attributed to

the El Niño or warm phase include (Bernal *et al.*, 1982; Blanco and Díaz, 1985; Fonseca, 1985): enhanced poleward transport of warm, saline water of equatorial origin at the surface and in the poleward undercurrent, high sea levels and SST, and low oxygen concentrations. Equatorial waves also propagate into the region as coastal trapped waves with periods of 5-50 days (Enfield *et al.*, 1987; Shaffer *et al.*, 1997). The poleward advection of equatorial water at the surface (due to waves or increased poleward currents) depresses the thermocline and nutricline, thus reducing primary productivity. Although the relationship between oceanographic conditions and fish production is complex, El Niño periods tend to coincide with both a reduction in fish biomass and with changes in the dominant species from anchovy to sardine.

### **El Niño off Chile**

Philander (1990), Neelin *et al.* (1994), Battisti and Sarachik (1995), and Neelin and Latif (1998) review the equatorial dynamics of atmosphere and ocean associated with the ENSO phenomenon. Strub *et al.* (1998) summarize past observations of El Niño effects along the coast of Ecuador, Peru, and Chile. The physical aspects of interest include: (1) changes in sea level and currents; (2) changes in the distributions (horizontal and vertical) of water properties; (3) the connection between local conditions and local and distant forcing; and (4) links to the biology. Here we consider the first three, reserving a description of the biological conditions for a separate analysis.

The connection between changing coastal conditions off Ecuador, Peru, and Chile and equatorial waves and currents was clearly established during the 1982-1983 El Niño.

Increased SST and depth of isotherms along the equator at 82.5°W preceded changes in October 1982 at 2°S (La Libertad) by two months (Cucalon, 1987) and changes at 10°S off Peru followed within days (Smith, 1983; Huyer *et al.*, 1987). Off Chile, the event was tracked in sea level down the coast to at least 33°S (Fonseca, 1985; Bilbao, 1992). Tide gauge and current meter data have been used to connect coastal trapped waves (CTW) along Peru and Chile and the equatorial wave guide (Smith, 1978; Brink, 1982, Enfield *et al.*, 1987; Cornejo and Enfield, 1987; Shaffer *et al.*, 1997). Shaffer *et al.* (1997) recently identified CTWs with nominal periods of 5, 10, and 50 days in current meter records along the Chilean continental slope at 30°S and found a connection with currents and winds 15,000 km away on the equator at the international date line. CTWs are thought to increase in strength during the onset of El Niño events (Enfield *et al.*, 1987; Shaffer *et al.* 1997).

Persistent and strong currents, associated or not with waves, are capable of advecting water masses long distances. The onset of El Niño off Peru is signaled by increased poleward currents for approximately 2 months. The average current speed over the shelf at 55 m depth during the El Niño period of April-May 1976 at 15°S was 23 cm s<sup>-1</sup> compared to 9 cm s<sup>-1</sup> during a similar period a year later (Smith, 1983). Similarly, currents over the shelf at 100 m depth at 10°S increased to 25 cm s<sup>-1</sup> during October-November 1982, compared to 4 cm s<sup>-1</sup> the previous year (Smith, 1983). The accelerated flow translates over a 2-month period to an increased displacement of 700-1000 km (7°-10° of latitude).

Changes in the distribution of water properties result from the horizontal and

vertical displacement of water masses. Blanco and Díaz (1985) documented the appearance off northern Chile of warmer and saltier surface water in December 1982 and its disappearance in December 1983. Fonseca (1985) traced increased SSTs at Chilean harbors to 35°S (Talcuahano) in early 1983. Lower oxygen concentrations along the coast were attributed to increased transport in the poleward undercurrent (Fonseca, 1985). This is consistent with the increased volume (and temperature) of ESSW (with respect to climatological values) from December 1982 to June 1983 off Antofagasta and Arica (Blanco and Díaz, 1985). Changes in vertical distributions are usually noted as displaced isotherms. Deepened surface isotherms were seen offshore at 10°S in November 1982 (Huyer *et al.*, 1987) and at 18°S, 20.5°S, and 24°S in December 1982 (Blanco and Díaz, 1985). An exact date of isotherm deepening is unknown as there were no transects for many months prior to November.

It was originally thought that changes in sea level and thermocline depth were caused by a decrease or reversal of local upwelling-favorable winds. However, measured winds off central Peru (Smith, 1983) during both the 1976 and 1982-1983 warm periods continued to be strongly equatorward. Equatorward winds at the coast actually increased at 12°S during the 1982-1983 event, but decreased at 5°S, responding to changes in the location of the ITCZ and the South Pacific High (Huyer *et al.*, 1987). Fonseca indicates that even though the South Pacific High weakened during parts of the 1982-1983 El Niño, Chilean coastal winds were still equatorward and therefore upwelling-favorable.

Below we examine the changes in forcing and ocean conditions off northern Chile

during the 1996-1998 period. Quarterly surveys carried out by the Chilean Fisheries Institute, IFOP (Instituto de Fomento Pesquero), allow a more detailed analysis than was previously possible. Likewise, a recently compiled hydrographic climatology, consisting of 30 years of physical conditions and circulation (Blanco *et al.*, 2000), provides a basis against which to quantify the magnitude of the observed changes. Section 2 describes the sources of data used in the study. The results are presented in Section 3, followed by discussion in Section 4 and a summary in Section 5.

## 2. Data and Methods

### Hydrographic Surveys

IFOP presently makes quarterly hydrographic surveys off northern Chile between 18°S and 24°S (Figure 1). This study focuses on data from 9 of these cruises (May 1996 to May 1998) during which 7 stations are occupied along each of 5 offshore transects separated by 148 km (35 stations total). Stations were located 1.8, 9.2, 18.5, 37, 74, 129.6, and 185 km from the coast. Temperature and salinity were measured continuously to 500 db with a SeaBird CTD (model 19) equipped with a General Oceanics rosette with 12 Niskin bottles of 1.7 l. Oxygen concentrations were calculated using the modified Winkler titration method. Salinities measured with Autolab induction salinometers from water samples collected at standard depths and temperatures from reversing thermometers were used to calibrate the CTD. Over 30 years (1964-1996) of data collected in similar surveys were used to calculate a climatological mean to quantify of



anomalous conditions. Since the sampling period spanned the three El Niño events as well cold periods (*e.g.*, 1988), the climatological mean is representative of both ‘normal’ and anomalous conditions. Blanco *et al.* (2000) present the three-month (seasonal) climatology of the region. Anomalies of the variables for the nine cruises discussed here were calculated using a monthly climatology of the 30-year data set (Blanco, 1996) to minimize possible noise due to the cruise occurring at the beginning or end of a season.

### **Time Series from Coastal Locations**

Wind speeds from 1970-1998 were obtained from the Dirección Meteorológica de Chile for airports located near Arica (18.5°S), Iquique (20.5°S), and Antofagasta (23.5°S). Monthly sea surface heights (1975-1998), adjusted for the inverse barometer effect, were obtained from the University of Hawaii Sea Level Center for tide gauges at Arica and Antofagasta. Monthly sea surface temperatures (SST) calculated at Arica, Iquique, and Antofagasta during 1960-1997 were provided by the Servicio Hidrográfico y Oceanográfico de la Armada de Chile. The climatological monthly means of these variables (Blanco *et al.*, 2000) were used here to form anomalies for the period between 1980-1998. These coastal time series place the hydrographic surveys in the context of the evolution between La Niña and El Niño conditions.

The best oceanographic temporal context, however, is provided by a time series of vertical profiles of temperature, measured approximately 10 km offshore of Iquique, in water over 500 m deep. Profiles are obtained every 2-4 weeks (more frequently when El Niño events are recognized). This invaluable time series of profiles has been maintained

by the IFOP with assistance of personnel at the Universidad Arturo Prat (arrows in Figure 2b indicate sampling times).

### 3. Results

#### Coastal Time Series

Monthly sea level anomalies from tide gauges located along the South American coast between the equator and  $37^{\circ}\text{S}$  for the period 1980-1998 (Figure 2a) do not allow analysis of phase propagation but clearly reveal the strength and extent of persistent sea level changes. The 1997-1998 and 1982-1983 El Niños were the dominant events in this period and were comparable in magnitude and duration. In each case, sea level anomalies exceeded 25 cm off Peru and northern Chile. In both events two sea level maxima were separated by a relaxation period. Though sea level anomalies were greater than 10 cm between the equator and  $37^{\circ}\text{S}$ , they were most pronounced north of  $20^{\circ}\text{S}$ .

Iquique ( $20.5^{\circ}\text{S}$ ), in the center of our region of interest, is at the southern limit of the stronger and more persistent sea level response in 1997-1998 (Figure 2a). The time series of temperature profiles from Iquique is presented in Figure 2b as a time-depth plot, using the same time axis. The two largest and most persistent disturbances in subsurface water properties occurred during the 1982-1983 and 1997-1998 El Niños. These data must be interpreted with some caution given uneven sampling frequency. Sampling was unfortunately sparse during the 1982-1983 event with only 9 cruises between January 1982 and December 1983. The 1997-1998 El Niño was better sampled

and 30 profiles were obtained between January 1997 and September 1998. The isotherms deepened with the two sea level maxima, in mid-1997 and again at the end of 1997 and beginning of 1998. In late 1997, the 15°C isotherm was deeper than 250m, its most extreme depth value on record.

Monthly anomalies of adjusted coastal sea level, coastal SST, and winds for the 1980-1998 period at locations between 18°-24°S are shown in Figure 3a. Sea level and SST anomalies from the northern and southern boundaries of the domain were greatest during the 1982-1983 and 1997-1998 events, as expected from Figure 2. However, the alongshore wind speed anomaly from Iquique only surpassed 1 m s<sup>-1</sup> in 1982-1983: the anomaly was upwelling-favorable in late 1982 in the first period of high sea level and downwelling-favorable in 1983 during the second maximum. Minimum average alongshore winds from the climatology (which occur in winter) are 2.5 m s<sup>-1</sup> (Blanco *et al.*, 2000), so anomalies below 2 m s<sup>-1</sup> (Figure 3a) can enhance or reduce upwelling, but cannot lead to downwelling.

Although monthly averages cannot clearly distinguish the El Niño signal from intraseasonal variability due to coastally-trapped waves, we present them below to provide a context to the observed hydrographic changes. The expanded view of 1995-1998 (Figure 3b) indicates that although two distinct maxima occurred in SST at the three coastal stations, the relaxation between the peaks in sea level was not clear in the north (Arica). SST maxima were almost synchronous at the three locations and followed those of sea level by one to two months. Wind anomalies were moderately upwelling-favorable (in the south) or weak at the onset of the first pulse in May 1997,

then became mildly downwelling-favorable in the northern half of the domain (Arica and Iquique) until the relaxation. Continued moderately downwelling-favorable wind anomalies at Arica may explain the lack of a relaxation in sea level there. During the second pulse (December 1997 - January 1998) the downwelling-favorable wind anomalies in the north cannot account for the onset of high sea levels and SSTs in May, although it may have enhanced the signal in the north after the first pulse and limited the relaxation. The normal summer winds during December 1997 - March 1998 in the southern part of the domain cannot account for the observed anomalies in sea level, SST, and isotherm depth during the second pulse. Comparable wind anomalies in preceding years (all of 1984 and early 1985 in Figure 3) were accompanied by moderate depressions in the 13°C isotherm, and a smaller effect on the 15°C isotherm. These factors point to non-local forcing as the cause for the observed anomalies.

Observations along the equator in the Eastern Pacific reveal that pulses of high SSTs and depressed isotherms arrived off the coast of Ecuador in March 1997 (briefly), May-August 1997 and October 1997 - February 1998 (Chávez *et al.*, 1998). The timing of the pulses of high sea level and SST off northern Chile is consistent with an equatorial source in May-August and November-February.

The best evidence for an equatorial connection comes from temperature profiles and tide gauge sea levels from Peru and Chile. Elevated daily sea levels (not presented) at the beginning of May 1997 propagated poleward from Baltra (at the equator) to Talcahuano (37°S) in about 11 days, corresponding to an approximate phase velocity of 250-300 km day<sup>-1</sup>. By contrast to the transient event in March, sea levels remained

persistently high for several months. The same timing in the depression of isotherms measured off Iquique at 20.5°S was observed in temperature profiles (not presented) from 1996-1998 off Ecuador at 2°S (La Libertad, data provided by INOCAR) and Peru at 12°S (Callao, data provided by IMARPE). All three time series show two pulses separated by a relaxation, although the pulses lasted somewhat longer at 2°S (CPPS, 1999). A similar sudden warming was also observed in early May 1997 in a bay north of Antofagasta, but the time series (to August 1997) ended before the relaxation and second pulse (Escribano, 1998). These signals followed those at the equator (Chávez *et al.*, 1998) supporting the connection to equatorial events. These data illustrate the need for time series of subsurface conditions to facilitate interpretation of surface signals (SST, sea level) that may respond rapidly to local forcing. The hydrographic cruises provide additional evidence on the role of CTWs.

### **Hydrographic Cruises Prior to and During the El Niño: May 1996 - March 1998**

Surface fields of temperature and salinity between May 1996 and March 1998 are shown in Figures 4 and 5 along with their associated anomalies. Figures 2 and 3 provide a temporal context for the surveys. The first three cruises (May, September, and December 1996) occurred during the low sea level, cold period (La Niña) prior to El Niño conditions while the March 1997 cruise corresponds to transitional sea levels and coastal SSTs. May and December 1997 surveys were made during the first and second pulse of high sea level respectively, and August 1997 was either near the end of the first

pulse in sea level or in the relaxation period. In March 1998, sea levels at Antofagasta had returned to normal, although sea levels at Arica and coastal SST values throughout the region were still high. By May 1998, sea levels and SSTs were again below the climatological mean, similar to those of 1996 prior to the onset of El Niño.

The seasonal progression of SST patterns (Figure 4a) from May 1996 to March 1997 was approximately normal: the offshore gradient disappeared and the north-south gradient weakened in winter (September 1996) and both were re-established in spring and intensified in summer (December 1996 - March 1997). However, the surface was generally cooler ( $-1$  to  $-3^{\circ}\text{C}$ ) (Figure 4b). The temperature anomalies were consistent with less equatorial water (STW) offshore (e.g. in the northeast in May 1996) and stronger upwelling in the center of the domain (maximum in December 1996 and March 1997). In March 1997, the  $23^{\circ}\text{C}$  and  $24^{\circ}\text{C}$  isotherms extended further south than climatology, leading to a weak positive SST anomaly and a stronger cross-shelf gradient than usual.

May and August 1997 SSTs were approximately  $3^{\circ}\text{C}$  warmer than the previous year. By May 1997 offshore SST exceeded  $21^{\circ}\text{C}$  throughout the domain (Figure 4a), creating positive anomalies of  $1$ - $3^{\circ}\text{C}$  in the south (Figure 4b). Typical fall upwelled water was absent except at  $21.5^{\circ}\text{S}$ , so coastal anomalies were approximately  $1$ - $2^{\circ}\text{C}$ . The disappearance of the meridional gradient led to stronger SST anomalies in the south. August 1997 presented the usual winter homogeneous SST field north of  $23^{\circ}\text{S}$ , but with higher temperatures ( $2$ - $3^{\circ}\text{C}$ ). In December 1997 the usual spring offshore gradient was essentially absent except at  $21^{\circ}\text{S}$ , consistent with ongoing upwelling. SST

anomalies ranged from 1° to 2-4°C. The gradient increased in March 1998, in response to offshore heating and coastal upwelling and the total area of anomalously warm water was reduced. Anomalies were minimum at 21°S but remained at 2°C or more to the south and north.

Climatological surface salinity patterns are similar to those of SST (Blanco *et al.*, 2000). From May 1996 through March 1997 the seasonal progression was normal (Figures 5a and 5b) with generally lower salinity values (anomalies of 0.1-0.3 practical salinity units or psu). The characteristic meridional salinity gradient (Blanco *et al.*, 2000) was observed, but the cross-shelf gradient was weak. Positive (in May 1996) or weak negative anomalies occurred close to the coast. Negative anomalies were strongest offshore (maximum in September 1996), consistent with the decreased influence of STW (similar to that inferred from the cool SST pattern).

The upwelling-induced cross-shelf gradient was close to normal in May 1997, but the salinity values were slightly above climatology, leading to positive anomalies (<0.1 psu) in most places. This cruise revealed a transition from cool and fresh to moderately warm and salty anomalies. The typical uniform winter pattern in August 1997 was restricted to the north; a meridional front near 21°S and anomalies of order 0.2-0.3 psu suggested increased poleward transport of STW. Upwelling re-established the offshore gradients in spring and summer (December 1997 and March 1998), but values remained anomalously high by 0.2-0.6 psu. Maximum anomalies occurred in the south in December 1997, reflecting the reduced north-south gradient.

Cross-shelf transects of the vertical distribution of temperature, salinity, and

oxygen at 21°S (Pta. Lobos in Figure 1), and the anomalies for temperature and salinity, changed significantly during the study period (Figures 6, 7, and 8). From May 1996 to March 1998 isotherms shoaling towards the coast indicate near-surface upwelling. From May to December 1996, the surface mixed layer was exceptionally shallow and temperatures in the upper 100 m were lower than climatology (Figure 6). The 13°C isotherm was shallower during this period than its usual upper limit of 100m (Blanco *et al.*, 2000). This shoaling of the thermocline led to maximum negative anomalies of 2-3°C at 30-50 m (Figure 6b), where the vertical temperature gradient is normally maximum. The poleward undercurrent, indicated by spreading isotherms between 12°C and 13°C, was stronger than normal during May 1996, creating weak positive anomalies below 200 m. The temperature structure below 100 m was similar to the climatology between September 1996 and March 1997, as indicated by anomalies of less than 1°C. In March 1997, a stronger and deeper thermocline offshore led to warm surface anomalies (>2°C).

By the time of the first sea level peak in May 1997 the subsurface thermal structure had changed substantially. The 13°C reached 200 m at the coast, though it was close to normal 150 km offshore. The undercurrent appeared to be strong, with maximum isotherm slopes approximately 100 km from the coast. Anomalies of over 1°C extended to 500 m inshore of 100 km. The anomaly at 40 m depth (2-3°C) was greater than at the surface (Figure 4b). During the relaxation between pulses (August 1997), the isotherms were level and positive anomalies (2-3°C) were restricted to the upper 100 m (Figure 3b). December 1997, during the second sea level maximum, presented the



most extreme anomalies at depth. The undercurrent was relatively strong, with steepest isotherm slopes at approximately 100-200 m depth within 100 km from the coast. Near-shore temperature anomalies surpassed 2-3°C to 300 m. Offshore stratification was enhanced at the thermocline (30- 50 m), creating anomalies of 3-4°C. In March 1998, the undercurrent was reduced or absent and the entire water column below 100 m was 2°C cooler than in December. Anomalies below 200 m had reversed to become weakly negative although high positive anomalies (4-5°C) persisted in the upper 100 m. Generally, the intensity and extent of the subsurface anomalies did not correspond directly to the those at the surface (Figures 4b and 6b).

The salinity transects, though generally similar to those of temperature, help clarify water mass distributions (Figure 7a). In May 1996 the salty STW (here only slightly over 35.0) could be distinguished at the surface in the offshore region. SAW (34.4-34.5) was found underneath the STW offshore, while relatively salty ESSW (34.9) was found near the coast between 100-300 m in the undercurrent and upwelling into the upper 50 m. From May to December 1996, both STW and SAW were fresher than climatology, leading to negative salinity anomalies of up to 0.4-0.5 at 30-50 m (Figure 7b). The anomalously fresh intrusion of SAW continued through December of 1996, almost reaching the coast in the upper 100m. In September and December 1996 no STW water was evident above SAW. The salinity maximum of the undercurrent in December 1996 was weaker than the climatological spring field, producing negative salinity anomalies next to the coast at depth. In March 1997 salinities were close to summer climatology with patchy and weak negative anomalies in the upper 100 m.

In May 1997 anomalies over most of the water column changed from weakly negative to positive, concurrent with those of subsurface temperature (Figures 6 and 7). An intensified and shallow undercurrent brought saltier ESSW (34.9-35.0) into the region within 100 km of the coast, while a deep layer of STW ( $>35.0$ ) extended throughout the transect. The fresh tongue of SAW in the west was depressed by the increased volume of STW and its eastward progression was limited by the undercurrent. Anomalies were positive in the upper 50 m through the transect and within 125 km of the coast to 500 m depth, while negative anomalies were found offshore at 75-100 m (Figure 7b). During the relaxation in August 1997 the surface layer was deeper and more saline, creating positive anomalies of 0.3 psu in the upper 50 m. As in temperature, December 1997 presented the greatest changes at depth, with positive salinity anomalies to 400-500 m near the coast and to 100 m offshore. In December 1997 a tongue of STW (35.5) penetrated the upper 50 m, surfacing within 50 km of the coast in March 1998. Maximum anomalies (0.5-0.6) were observed offshore of 100 km in the upper 50 m in December 1997 and March 1998. Nearshore, upwelling of fresher water reduced the anomalies to 0.2-0.3. SAW was present at greater depths than usual in the offshore half of the transect, creating negative anomalies (0.1-0.2) slightly below 100 m depth. In March 1998 the upper 80 m were anomalously saline (STW). Below this, the water column was fresher than climatology due to a decrease in the undercurrent.

The climatological seasonal variation in oxygen concentrations in the upper 100 m is weak (Blanco *et al.*, 2000). Values surpass  $5 \text{ ml l}^{-1}$  in a 50 m deep surface layer 400 km offshore and shoaling to the surface at the coast. The  $0.5 \text{ ml l}^{-1}$  isopleth is found

at 125-150 m offshore and shoals to 75-100 m at the coast; this slope increases slightly in spring and summer. Minimum oxygen concentrations ( $< 0.5 \text{ ml l}^{-1}$ ) occur between 125 and 450 m in the ESSW carried by the poleward undercurrent. From May 1996 to March 1997 the vertical gradient in oxygen concentration above 100 m was enhanced due to the combined effect of high subsurface oxygen, associated with onshore penetration of SAW, and an intensified undercurrent (Figure 8). The  $0.5 \text{ ml l}^{-1}$  isopleth was above 100 m due to the increased volume of low oxygen ESSW.

In May and December 1997 and March 1998 the surface layer of high oxygen concentrations deepened to 100-150 m, as STW and SAW extended from offshore to the coast. In August 1997, during the relaxation between pulses, the low oxygen concentration core shoaled and the upper layer of high oxygen concentrations thinned to less than 100 m. During the El Niño period (May 1997 to March 1998) the vertical gradient was weaker than the previous year as both STW and SAW overlaid the ESSW.

T-S diagrams from the transect at  $21^{\circ}\text{S}$  from each cruise summarize the relative influence of the different water masses (Figure 9). Between May and December 1996, there was a much stronger influence of SAW (the subsurface relative minima in salinity) and a weaker influence of STW than is usually found at this latitude (Blanco *et al.*, 2000). The seasonal progression resembled more closely that normally observed further north in sections off Antofagasta at  $23^{\circ}\text{S}$  (Blanco *et al.*, 2000). There was virtually no STW in September and December 1996. The T-S characteristics of March 1997 represent a transition between La Niña and El Niño conditions and resembled climatological values at this latitude, except for a stronger influence of SAW in the most

offshore profiles and a warmer, more saline upper layer.

In May 1997 the T-S characteristics of the upper layer reflect the influence of STW and resembled the climatological T-S characteristics from Arica, to the north. SAW remained (as a mid-depth minimum in salinity) through March 1998 in the offshore profiles. Though salinity values corresponded to SAW at this latitude, the temperature was higher and the thickness of the layer (temperature range) was less than in the seasonal climatology (Blanco *et al.*, 2000). From May 1997, the upper part of the water column became progressively warmer and more saline. By March 1998, the T-S values were close to those of pure STW and much higher than those of the modified STW usually found in this region. The ESSW was warmer and shallower than usual from May 1997 to March 1998. The characteristic salinity maximum due to ESSW disappeared as the salinity increased in the upper part of the water column. Results for May and August 1998 are discussed later.

Geopotential anomalies (scaled like dynamic heights) at the surface and at 200 db relative to 500 db portray surface and subsurface (200 m) circulation respectively (Figures 10a and 10b). Surface flow was primarily equatorward from May 1996 through March 1997. Equatorward flow was stronger in the north than in the south during May 1996 and March 1997. In September and December 1996, equatorward flow within 100 km of the coast was stronger and more uniform throughout the study region than in the climatology (Blanco *et al.*, 2000). This is consistent with the colder, fresher water in the surface layers (more SAW, less STW). During the same period (May 1996 through March 1997) flow at 200 m was primarily poleward, strongest in May 1996 and March

1997 (Figure 10b). The increased poleward flow in March 1997 corresponds to the seasonal progression, as the undercurrent maximum is in summer (Blanco *et al.*, 2000). Stronger poleward flow in May 1996 is consistent with the increased thickness of the salty undercurrent (Figures 6a, 7a, and 9).

In both May and December 1997 (the two sea level peaks), strong poleward currents were found at both the surface and at 200 m (Figure 10), with onshore flow in the north of the domain. This is consistent with the increased volume of STW at the surface and with the subsurface layer of SAW stretching onshore in the north. In contrast, the relaxation period (August 1997) presented equatorward flow in the center of the domain, onshore flow in the south, and offshore flow in the north. The currents in the upper 200 m switched from relatively baroclinic (opposite directions at the surface and at 200 m) during the year preceding the El Niño, to relatively barotropic (currents in the same direction) during the sea level pulses and immediately following them. In March 1998, the flow was strongly equatorward in the northern and southern parts of the domain and there was no poleward component, although the climatological undercurrent maximum is in summer. This is consistent with weak ESSW, collapse of the oxygen minimum, and minimum cross-shelf slope of isotherms and isohalines.

Temporal evolution of the vertical structure of alongshore velocity can be visualized in offshore sections of geostrophic velocity relative to 500 db (Figure 11). Flow in the year prior to the El Niño was generally weaker and more complex compared to that during the two pulses of high sea level in May and December 1997. May 1996 and March 1997 presented large vertical shear. Below 100 m, the flow was relatively barotropic,

with alternating cross-shelf bands of equatorward and poleward flow caused by eddies and meanders. During May and December 1997, strong poleward flow extended throughout the water column, with subsurface maxima of 20-35 cm s<sup>-1</sup> centered at 100 m. Following the poleward pulses, flow was again more complex and generally equatorward with maxima (relative to 500 m) of about 10 cm s<sup>-1</sup>.

### **Hydrography after the El Niño: May 1998**

By May 1998, alongshore winds, coastal sea levels and SSTs were near climatological seasonal mean values (Figure 3). The eastern equatorial Pacific was engaged in a rapid transition to La Niña conditions (Neelin and Latif, 1998). During the May 1998 cruise, SST and surface salinity adjacent to the coast approached normal seasonal values (anomalies <1°C, ~0.1 psu) due to coastal upwelling (Figure 12). SST was close to climatology in most of the region but offshore salinity, and nearshore at 19.7°S, was still very high (35.4-35.6). The largest anomalies (2°C and 0.5 psu) occurred 20-40 km offshore at 19.7°S. The surface and subsurface geopotential fields indicated that this patch was associated with strong onshore flow of warm, salty water at 20°-21°S around an anticyclonic eddy (Figure 12).

Cross-shelf sections of temperature, salinity, temperature anomaly, salinity anomaly, oxygen and alongshore geostrophic velocity at 21°S are presented in Figure 13, for comparison to Figures 6, 7 and 8. Unfortunately, these sections sample the southern edge of the eddy in Figure 12. The associated salinity anomalies do not extend below 30m depth. Similar sections at 19.7°S from the same survey (not presented) which

sampled the core of the eddy revealed a surface layer of STW 200km offshore leading to strong salinity anomalies extending to 100 m depth. At  $21^{\circ}\text{S}$ , temperatures below 50 m were close to the fall average conditions, while salinities and temperatures between 25 and 50 m were fresh and cool (Figure 13), likely of SAW origin, perhaps carried onshore along the southern flank of the anticyclonic eddy. The poleward flow along the coast at  $21^{\circ}\text{S}$  (Figure 13) was not part of a continuous undercurrent but of a southward meander visible in the horizontal geopotential fields. The T-S diagrams corresponding to  $21^{\circ}\text{S}$  in May 1998 (Figure 9) continued to present surface STW, the SAW relative salinity minimum, and a weak ESSW signature, consistent with the absence of poleward flow.

Thus, although the general return to climatological conditions is clear in May 1998, the offshore and northern part of the study region was dominated by a strong anticyclonic eddy. A larger-scale survey (not presented) revealed a tongue of surface STW extending southeast along the Peruvian coast (Blanco *et al.* 1999a). The eddy in the northern part of Figure 12 is part of a larger and stronger eddy centered to the north of the study region ( $\sim 18^{\circ}\text{S}$ ,  $72^{\circ}\text{W}$ ) which appeared to be in the process of separating from the tip of that tongue.

The IFOP survey in August 1998 found normal SST over most of the study area. Nearshore SST and salinities were low (by  $1\text{-}2^{\circ}\text{C}$  and  $0.1\text{-}0.2$  psu) due to strong upwelling. Positive salinity anomalies in the northwest corner dropped to about  $0.1\text{-}0.2$  psu. T-S curves from August 1998 along  $21^{\circ}\text{S}$  indicated no salinity values above 35.0, a large volume of SAW, and a weak presence of ESSW (Figure 9). Finally, a cruise in December 1998 found no sign of the warm, salty patch in the northwest.

## 4. Discussion

### Comparison to 1982-1983

Anomalies in sea level and SST (Figure 3) as well as of temperature with depth (Figure 2) in the 1997-1998 El Niño off northern Chile were similar in magnitude to those in the 1982-1983 event. The El Niño of 1986-1987 was weaker and that of 1991-1992 shorter in duration. Both the 1982-1983 (Huyer *et al.*, 1987; Fonseca, 1985) and 1997-1998 El Niño events consisted of two distinct sea level maxima (Figure 3), although the seasonal timing of the two pulses differed. If we consider the high sea levels and depressed isotherms during December-January in each event as representative of the classic El Niño timing, the ‘other’ pulse arrived afterwards in 1982-1983, while in 1997 the ‘other’ pulse arrived earlier.

Sampling off Iquique during 1997-1998 (arrows in Figures 2 and 14) and the IFOP cruises covering 18°-24°S captured both pulses and the relaxation periods. During 1982-1983, the sampling at Iquique was not frequent enough to separate the pulses. However, IFOP cruises were carried out in April and December 1982, March, May-June, August-September, October, and December 1983 (Blanco and Díaz, 1985; Kelly and Blanco, 1986). In April 1982 conditions were similar to December 1996 and March 1997, i.e. cool and fresh. East of 72°W the temperature anomalies were negative ( $\sim 1^{\circ}\text{C}$ ), salinities was low ( $< 35$ ), and surface geostrophic velocities were equatorward. The 15°C isotherm at 20.5°S was at 50 m offshore and shoaled toward the coast. In December 1982, during the first high sea level pulse, surface geostrophic velocities were



strongly poleward from Arica to Antofagasta and the 15°C isotherm was depressed to 100 m offshore and to 150 m at the coast. Temperature anomalies exceeded 3°C east of 73°W in the north and 72°W in the south. Salinity was greater than 35.3 offshore north of Iquique and values below 35.0 were only found south of Antofagasta. Conditions in December 1982 resembled those of May 1997, though more extreme. During the relaxation in March 1983, the 15°C isotherm off Iquique was between 50-100 m, shoaling toward the coast and surface geostrophic velocities were equatorward. SST anomalies of 4°C extended as far south as Antofagasta. Surface salinities were 35.6 offshore of Iquique and 35.3 at Antofagasta. March 1983 was comparable, with stronger anomalies, to August 1997. The second sea level maximum in May-June 1983 was accompanied by a deepening of the 15°C isotherm at Iquique to 100 m. The survey revealed that surface geostrophic velocities were poleward, temperature anomalies exceeding 6°C north of 20°S and 4°C north of Antofagasta, and patchy salinities (35.3-35.6) north of Antofagasta. These conditions were comparable to those found in December 1997. IFOP surveys off northern Chile from August 1983 onward found generally equatorward surface geostrophic velocities and isotherms at normal depths. Positive anomalies in both surface temperature (1–2°C) and salinity (0.3 psu) persisted in the northwest corner of the study area until about June 1984. Thus, the evolution of hydrographic conditions during the 1982-1983 El Niño was similar to that encountered in 1997-1998.

In the 1997-1998 El Niño oxygen concentrations were above normal at the coast, as seen in the deeper than climatology 1 ml l<sup>-1</sup> oxygen isopleth (<100 m) during the surveys in May, December 1997, and March 1998 (Figure 8). The depressed oxygen

minimum can be explained by the increased volume of STW and the presence of SAW at mid-depth despite intensified poleward flow. Escribano (1998) observed increased oxygen concentrations concurrent with a sudden increase in temperature in the upper 80 m in May 1997 in a bay north of Antofagasta. By contrast Fonseca (1985) reported anomalously low oxygen concentrations in December 1982, both at the surface (slight) and at 100 m (anomalies of 0.6-1.2 ml l<sup>-1</sup>); the largest anomalies occurred offshore and to the south. Fonseca (1985) inferred that the decreased oxygen concentrations were due to enhanced transport in the undercurrent, as the low oxygen requires a northern origin. This is consistent with the increased volume and shallower position of warmer ESSW water seen in the T-S diagrams corresponding to December 1982 through December 1983 (Blanco and Díaz, 1985). Likewise the influence of SAW in 1982-1983 appeared to be less than climatology except towards the end of the event (September 1983 or later). Cruise data indicate that the nearshore oxygen minimum was deeper than usual in 1982 and 1983 (Kelly and Blanco, 1984). Morales *et al.* (1996) reported that the layer of low dissolved oxygen (<1 ml l<sup>-1</sup>) was shallower during cold or La Niña years, which is consistent with the observations from May 1996 through March 1997 (Figure 8).

### **The role of CTWs in the observed hydrographic changes**

The initial rise in sea level during the 1997-1998 El Niño appears to have propagated poleward with the appropriate speed for a CTW. The same is true of other shorter period disturbances, including the more transient March sea level rise. However, conditions found during and following the pulses off northern Chile differed from the observations

of Shaffer *et al.* (1997) in 1991-1992 in which the waves showed an approximate period of 50 days and a 50km offshore decay scale for velocity. The poleward currents in May and December 1997 (Figures 10 and 11) extended much further offshore than 50 km and the May velocity maximum was displaced from the coast, unlike the theoretical wave structure. The period suggested by the isotherms off 20.5°S (pulses of 3-4 months, separated by 2-3 months) is much longer than 50 days and more like a semi-annual period, although there may be 50-day signals that were not well sampled. From theory (Gill and Clarke, 1974), we expect the coastal ocean to adjust its circulation in response to changing forcing through the propagation of a series of CTWs of higher and higher modes. The arrival of the high sea level in May 1997 would be the first of these modes, beginning a process in which the regional circulation off northern Chile was modified for periods longer than those of the waves (the two sea level maxima and large-scale poleward flow). The severe displacement of the isotherms and isohalines within 50 km of the coast off Iquique in the December 1997 transects (Figures 6a and 7a) may include the signature of a passing low frequency CTW, associated with poleward flow and high sea levels.

During the periods of persistent poleward velocities, water with STW characteristics was advected southward and onshore thus changing water properties off northern Chile over a period of several months. The gradual shift in water mass properties, compared to the rapid increase in sea level and depression of isotherms, is seen in the increased anomalies of temperature and salinity between sea level maxima from May to December 1997. Velocities of 20-35 cm s<sup>-1</sup> (Figure 11) over a month correspond to displacements

of 500-900 km ( $5^{\circ}$ - $9^{\circ}$  of latitude). These velocities are comparable to those measured over periods of 2 months at the onset of the 1982-83 El Niño off Peru (Smith, 1983). The relaxation velocities (equatorward following the sea level maxima) are only one-half to one-third as large (Figure 11). Assuming the lower estimate of velocity and that the velocities lasted for two months, the water found off northern Chile at the end of the first pulse would have originated 1000 km to the north; it would have traveled half that distance north during the relaxation, and then moved another 1000 km to the south during the second pulse. With a net displacement of 1500 km, the water found off northern Chile in March 1998, would have a Peruvian source at approximately  $10^{\circ}\text{S}$ . An equatorward flow of  $10 \text{ cm s}^{-1}$  would require approximately 6 months to restore this water to its original position. This is consistent with observations in August 1998 that were close to climatology. We take this as the simplest explanations for the observed conditions off northern Chile in 1996-1998.

## 5. Conclusions

1. Cool, La Niña conditions prevailed in 1996: sea level anomalies were moderately negative off Peru and weakly negative off Chile. Surface temperatures and salinities in the region, and to 100 m at  $21^{\circ}\text{S}$ , were cool and fresh. The circulation was generally equatorward at the surface and weakly poleward at 200 m. Equatorward currents in the 100 km next to the coast are consistent with an increase in SAW and a decrease in STW.

2. In March 1997, May-July 1997, and October-February (1997-1998), pulses of high SST and sea level propagated from east to west along the equator (Chávez *et al.*, 1998). High monthly sea level anomalies along the South American coast extended to 37°S in May-July and October-February.

The pulse of sea level in March 1997 was visible in the daily sea level records (not presented) though not in the monthly averages. Deeper isotherms and a 2°C temperature anomaly were observed in the upper 50 m at 20.5°S.

3. During the two sea level maxima, the deepened isotherms led to positive temperature anomalies of 4-6°C to 50-150 m depth and of 2°C down to 400 m. The hydrographic surveys show strong (20-35 cm s<sup>-1</sup>) poleward flow extending through the water column beyond 400 m. Both pulses were followed by weaker (10 cm s<sup>-1</sup>) equatorward flow.
4. The alongshore wind remained upwelling-favorable (equatorward) throughout the study period. Continued upwelling nearshore is reflected in the water properties. In the north and center of the region, alongshore winds were weaker than usual (though still upwelling-favorable) during the first sea level maximum and may have contributed to that signal and the weaker relaxation.
5. The water mass properties during the sea level peaks correspond to unmodified STW near the surface and increased temperature in ESSW below 100 m, consistent with the enhanced poleward flow. Increased onshore flow in the northern part of the region is reflected in a layer of SAW between 75 and 150 m that reaches the

coast in March 1998.

6. Although the timing of sea level maxima at the equator and along the South American coast is consistent with CTW propagation, the isotherm oscillations at Iquique suggest a period much longer than 50 days and the offshore structure of the velocity did not conform to that of CTWs. We propose that the sudden sea level changes and strong poleward velocities reflect the propagation of a series of higher mode CTWs.
7. The water mass properties became progressively more modified after the initial pulse in May 1997. This was a consequence of the advection STW and ESSW into the region during the periods of persistent poleward flow and their removal by the weaker northward transport during the relaxation and recovery periods.
8. By May 1998, flow was again equatorward next to the coast and SST had returned to the climatological mean over much of the region. Salinity remained anomalously high offshore and at 19.5°S at the coast, associated with an anticyclonic eddy. This eddy appeared to be a remnant of the thick layer of STW that moved southeast during the El Niño pulses.
9. Between August and December 1998, anomalous conditions disappeared. Thus warm El Niño conditions were observed off northern Chile for approximately 1-1.5 years.
10. Hydrographic conditions evolved during the 1982-1983 El Niño in a similar fashion

than in 1997-1998, although anomalies were larger in 1982-1983. April 1982 conditions were comparable to December 1996 and March 1997. The first sea level maximum in December 1982 was similar to that in May 1997. The observations for the relaxation in March 1983 correspond to those of August 1997. The second sea level peak in May-June 1983 was comparable to that observed in December 1997. In both events positive surface anomalies were more persistent in the northwest where they remained until June 1984 (August 1998).

### **Acknowledgments.**

Wind data were supplied by the Dirección Meteorológica de Chile and temperature data at coastal tide gauges came from the Servicio Hidrográfico y Oceanográfico de la Armada de Chile. Monthly sea levels at the tide gauges were obtained from the University of Hawaii. Data collection and support for JLB were provided by IFOP, with funding by the Fondo de Investigación Pesquera (Projects FIP 95-05, 96-07 and 97-02). Funding for travel for all authors to collaborate in the analysis of these data came from an NSF supplement to grant OC-9711344 (part of the US GLOBEC program). Additional funding for ACT came from NASA grants NAG5-6558 and NAG5-6604 and NSF grant OCE-9711919 (part of the US GLOBEC program). Additional funding for MEC was provided by the NASA Ocean Biogeochemistry Program and for PTS by JPL grant 958128 (TOPEX) and NASA grants NAG5-4947 (EOS) and NAG5-6604.

## References

- Bernal, P.A., F.L. Robles, and O. Rojas, 1982. Variabilidad física y biológica en la region meridional del sistema de corrientes Chile-Peru. *Monogr. Biol.*, 2, 75-102.
- Bilbao, P., 1992. Características físicas del fenómeno de El Niño 1982-1983 en la costa de Chile, Oceanography thesis, Universidad Católica de Valparaíso, Chile.
- Blanco, J.L., and M. Díaz, 1985. Características oceanográficas y desarrollo de El Niño 1982-83 en la zona norte de Chile, *Invest. Pesq. (Chile)*, 32, 53-60.
- Blanco, J. L., 1996. Variabilidad térmica y salina en la zona norte de Chile. IFOP data report.
- Blanco, J.L, L. Pizarro, T. De la Cuadra, G.A. Camacho., R. Martinez y J. Quintana, 1999a. Características meteorológicas y oceanográficas en el Pacífico Sudeste durante la declinación del evento El Niño 1997-1998. *Crucero Regional Conjunto*. Mayo 1998. Comisión permanente del Pacífico Sur. (In press).
- Blanco, J.L., A.C. Thomas, M.-E. Carr, and P.T. Strub, 2000. Seasonal climatology of hydrographic conditions in the upwelling region off northern Chile. (submitted to *J. Geophys. Res.*).
- Brink, K.H., 1982. A comparison of long coastal trapped wave theory with observations off Peru. *J. Phys. Oceanogr.*, 12, 897-913.
- Chávez, F.P., P.G. Strutton, and M.J. McPhaden, 1998. Biological-physical coupling in the central equatorial Pacific during the onset of the 1997-1998 El Niño, *Geophys. Res. Lettr.*, 25, 3543-3546.
- Cornejo, M.P., and D.B. Enfield, 1987. Propagation and forcing of high-frequency sea level variability along the west coast of South America, *J. Geophys. Res.*, 92, 14,323-14,334.
- CPPS, 1999. Informe final de la XIII Reunion del comité científico del programa ERFEN.



- Guayaquil, Noviembre, 1998. Comisión Permanente del Pacífico Sur. (In press).
- Cucalon, E., 1987. Oceanographic variability off Ecuador associated with an El Niño event in 1982-1983, *J. Geophys. Res.*, 92, 14309-14322.
- Enfield, D.B., 1981. Thermally driven wind variability in the planetary boundary layer above Lima, Peru, *J. Geophys. Res.*, 86, 2005-2016.
- Enfield, D.B., M.P. Cornejo-Rodriguez, R.L. Smith, and P.A. Newberger, 1987. The equatorial source of propagating variability along the Peru coast during the 1982-1983 El Niño, *J. Geophys. Res.*, 92, 14,335-14,346.
- Escribano, R., 1998. Population dynamics of *Calanus chilensis* in the Chilean Eastern Boundary Humboldt Current, *Fish. Oceanogr.*, 7, 245-251.
- Fonseca, T., 1985. Efectos físicos del fenómeno El Niño 1982-83 en la costa chilena. *Invest. Pesq. (Chile)*, 32, 61-68.
- Gill, A.E., and A.J. Clarke, 1974. Wind-induced upwelling, coastal currents and sea level changes, *Deep-Sea Res.*, 21, 325-345.
- Huyer, A., R.L. Smith, and T. Paluszkiwicz, 1987. Coastal upwelling off Peru during normal and El Niño times, 1981-1984. *J. Geophys. Res.*, 92, 14,297-14,307.
- IFOP, 1999. Investigación de la situación de las principales pesquerías pelágicas, Zona norte 1998. Instituto de Fomento Pesquero. Informe Final de Proyecto, 50 pp.
- Kelly, R., and J.L. Blanco, 1986. Características oceanográficas en el norte de Chile durante la declinación de El Niño 1982-83, *Invest. Pesq. (Chile)*, 33, 77-90.
- Morales, C.E., M. Braun, H. Reyes, J.L. Blanco, and A. G. Davies, 1996. ANchovy larval distribution in the coastal zone off northern Chile: the effect of low dissolved oxygen concentration and of a cold-warm sequence (1990-1995), *Invest. Mar. Valparaíso*

(Chile), 24, 77-96.

Neelin, J.D., M. Latif, and F.-F. Jin, 1994. Dynamics of coupled ocean-atmosphere models:

the tropical problem, *Annu. Rev. Fluid Mech.*, 26, 617-659.

Neelin, J.D., and M. Latif, 1998. El Niño dynamics, *Physics Today*, 51(12), 32-36.

Philander, S.G., 1990. El Niño, La Niña, and the Southern Oscillation. Academic Press, San

Diego, CA, 289 pp.

Shaffer, G., O. Pizarro, L. Djurfeldt, S. Salinas, and J. Rutllant, 1997. Circulation and

low-frequency variability near the Chilean coast: Remotely forced fluctuations during

the 1991-92 El Niño, *J. Phys. Oceanogr.*, 27, 217-235.

Smith, R.L., 1978. Poleward propagating perturbations in currents and sea level along the

Peru coast. *J. Geophys. Res.*, 83, 6083-6092.

Smith, R.L., 1983. Peru coastal currents during El Niño: 1976 and 1982, *Science*, 221,

1397-1399.

Strub, P.T., J.M. Mesias, V. Montecino, J. Rutllant, and S. Salinas, 1998. Coastal ocean

circulation off western South America, *The Sea*, 11, Robinson, A.R., and K.H. Brink,

273-313.

---

Received \_\_\_\_\_

**Figure 1.** Map of study region, transects, and stations for hydrographic cruises. The coastal time series was carried out off Iquique at 20.5°S.

**Figure 2.** (a) Time-latitude plot of monthly sea surface height anomalies from coastal tide gauges along the west coast of South American (locations at the right) from 1980-1996. Plus and minus indicate the sign of the anomaly; (b) time-depth plot of temperatures 10 km offshore of Iquique. Sampling is indicated by arrows.

**Figure 3.** (a) Monthly anomalies of sea level and SST at Arica and Antofagasta, and alongshore wind speed at Iquique for 1980-1998; (b) Monthly anomalies of the same variables for 1995-1998 from all three stations.

**Figure 4.** (a) SST from May 1996 through March 1998; (b) Anomalies of SST.

**Figure 5.** (a) Surface salinity from May 1996 through March 1998; (b) Anomalies of surface salinity.

**Figure 6.** (a) Cross-shelf temperature distribution along the transect at 21°S (Pta. Lobos) from May 1996 through March 1998; (b) Cross-shelf vertical distribution of temperature anomalies.

**Figure 7.** (a) Cross-shelf vertical salinity distribution along 21°S from May 1996 through March 1998; (b) Cross-shelf vertical distribution of salinity anomalies.

**Figure 8.** Cross-shelf vertical distribution of oxygen concentrations along 21°S from May 1996 through March 1998.

**Figure 9.** Temperature-Salinity diagrams for all stations along 21°S from May 1996 through August 1998.

**Figure 10.** (a) Geopotential anomaly at 0/500db from May 1996 through March 1998; (b) Geopotential anomaly at 200/500db.

**Figure 11.** Alongshore geostrophic velocities relative to 500db along the section at 21°S.

**Figure 12.** May 1998. Top: SST, surface salinity, geopotential anomaly (0/500). Bottom: SST anomaly, surface salinity anomaly, geopotential anomaly (200/500).

**Figure 13.** May 1998 sections at 21°S of temperature, salinity, geostrophic velocity relative to 500 db, salinity anomaly, temperature anomaly, and oxygen.

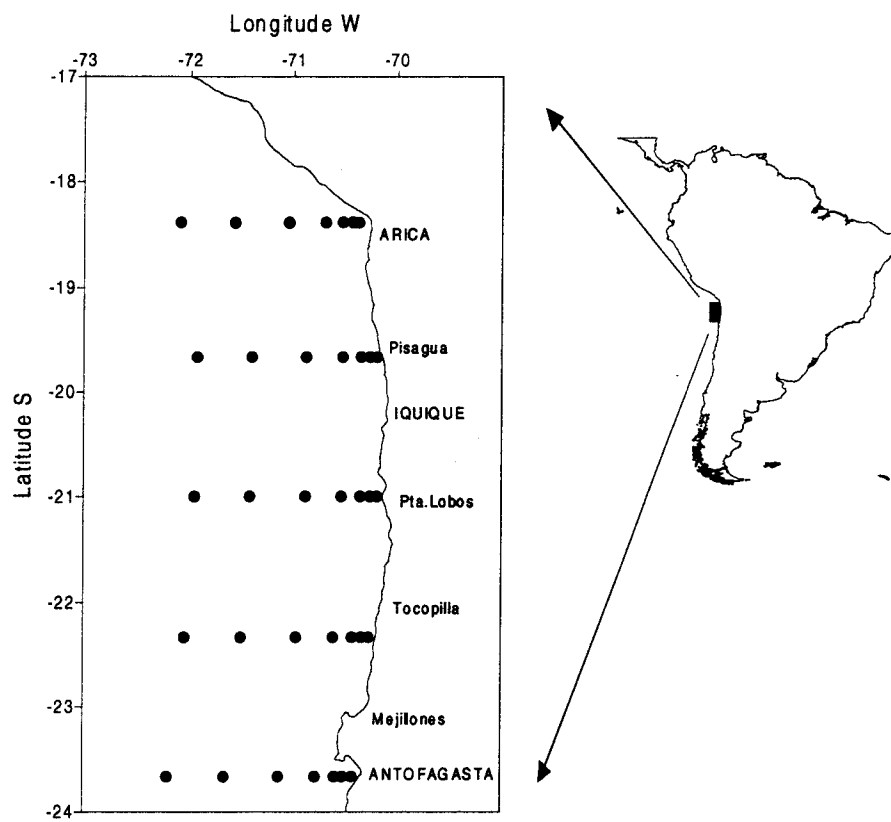


Fig. 1

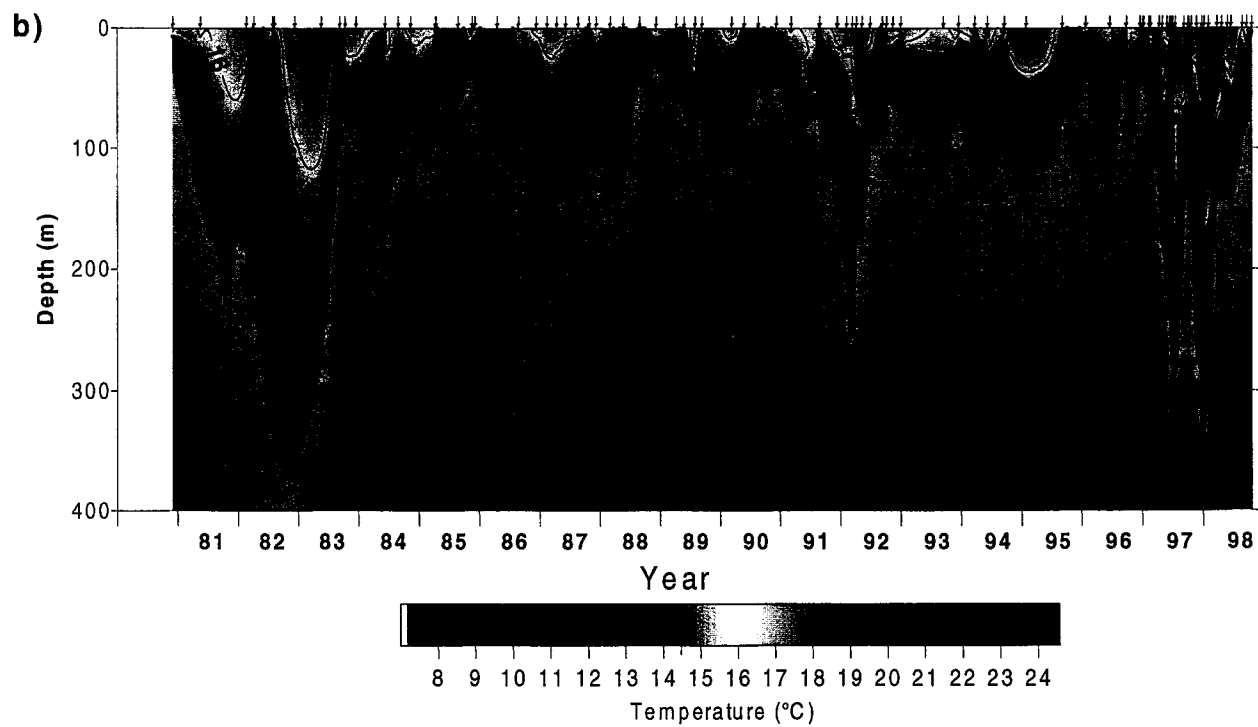
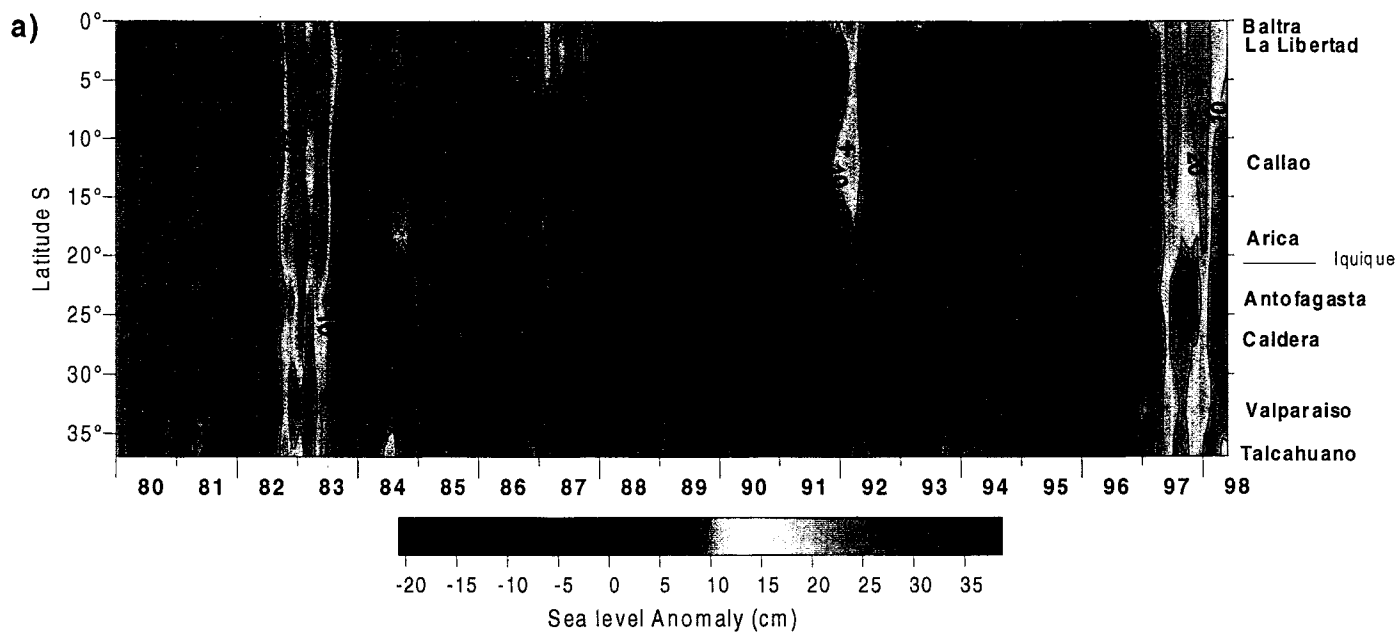


Fig. 2

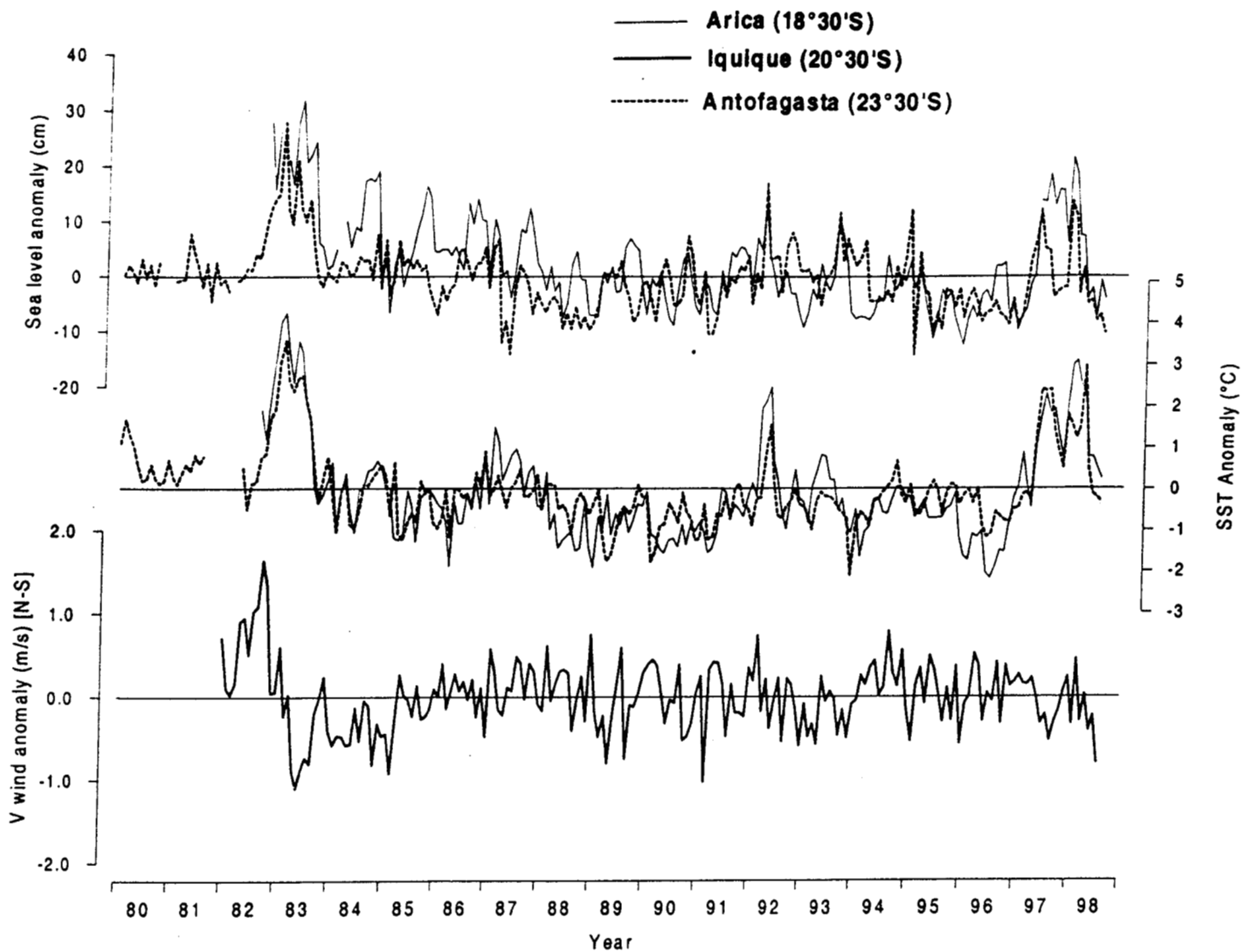


Fig. 3a

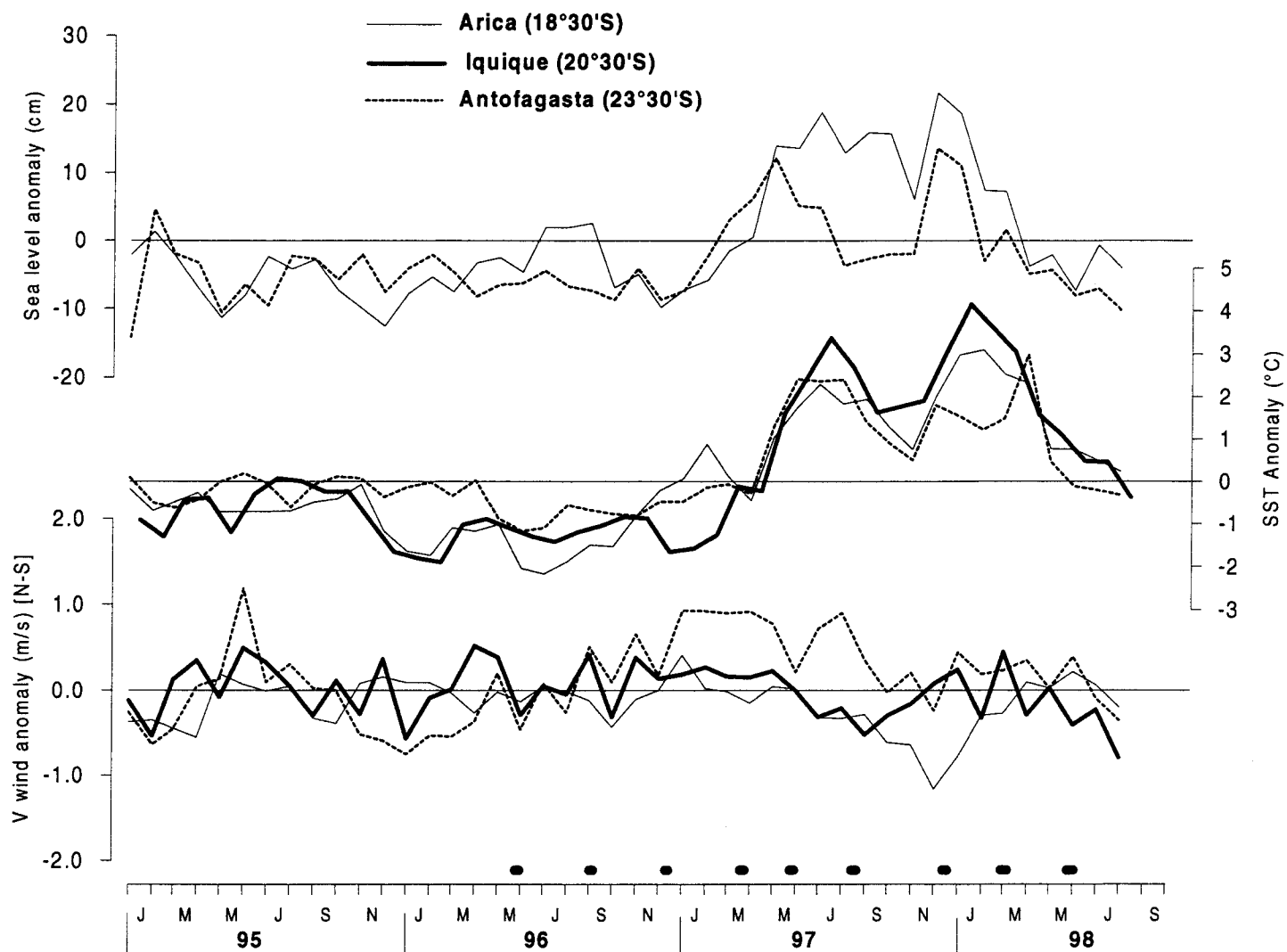


Fig. 3b



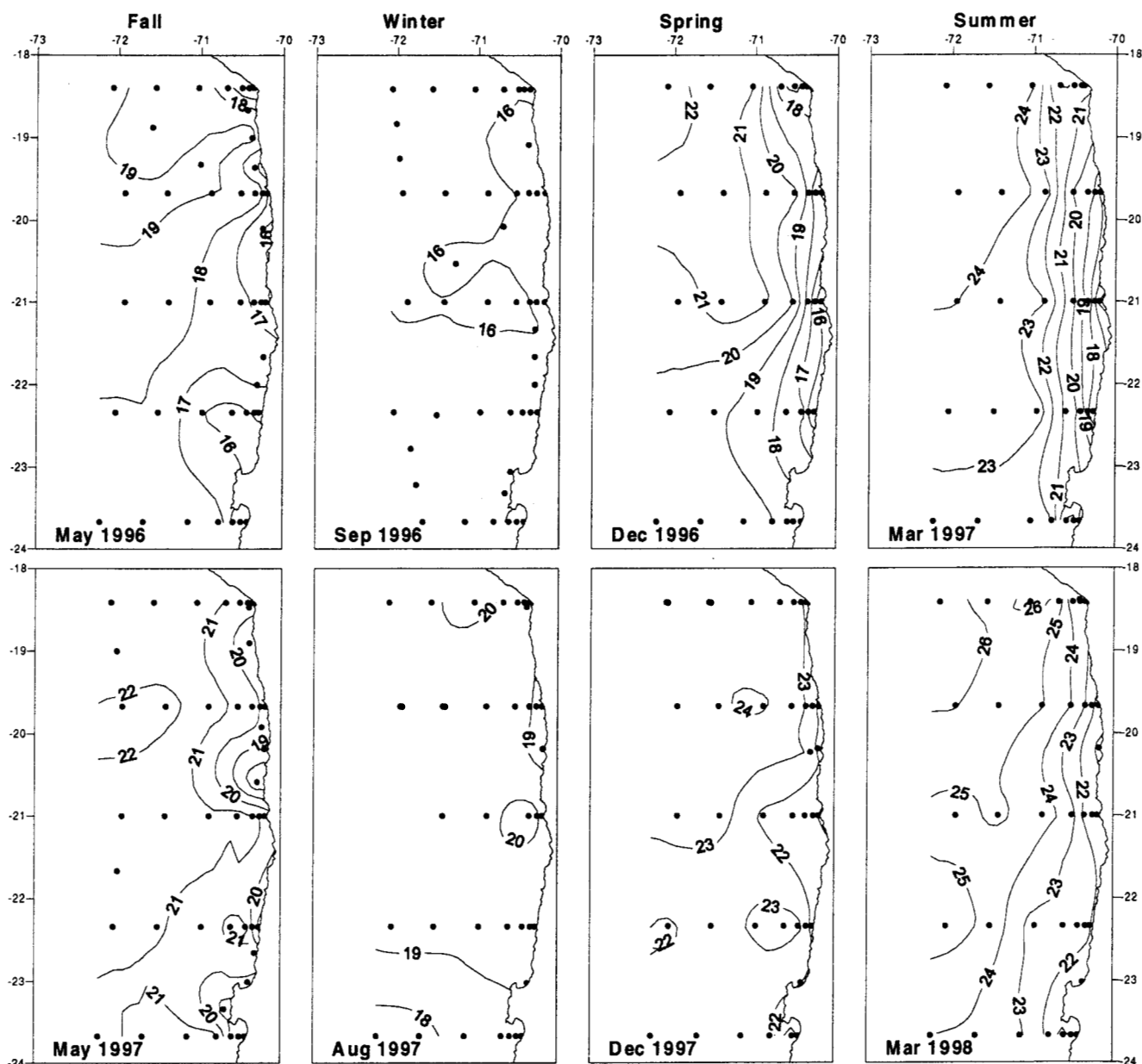


Fig. 4a

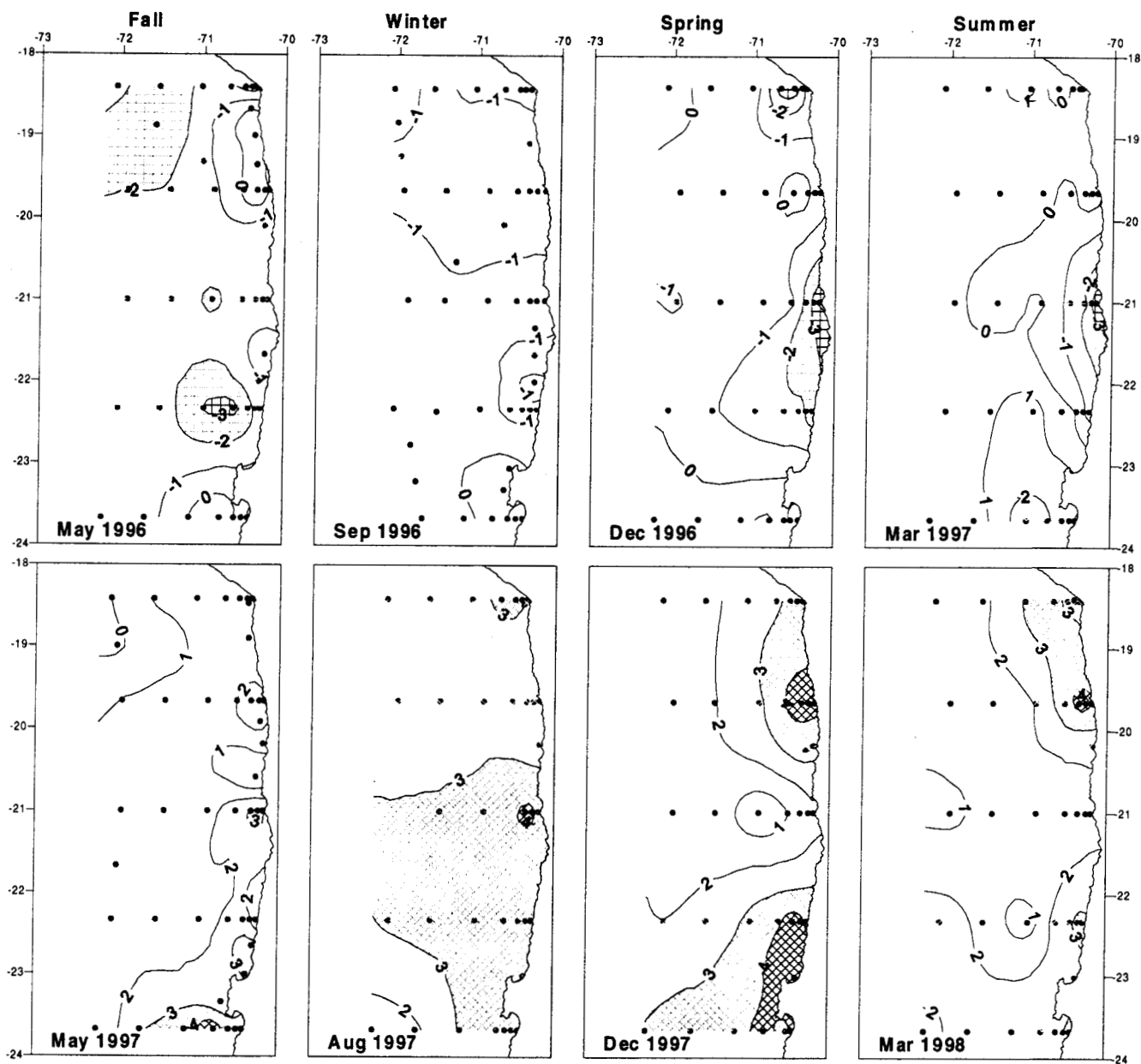


Fig. 4b

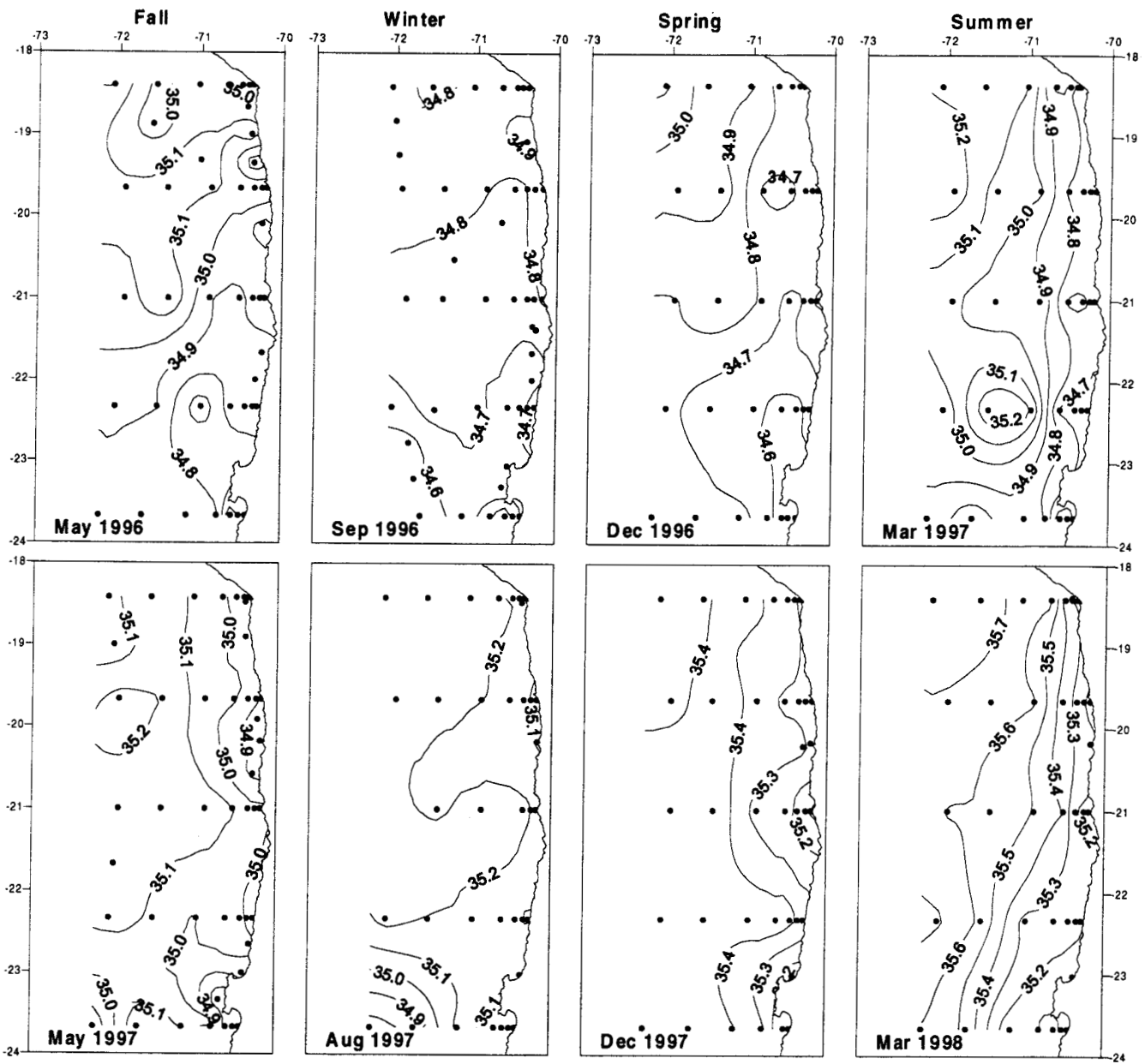


Fig. 5a

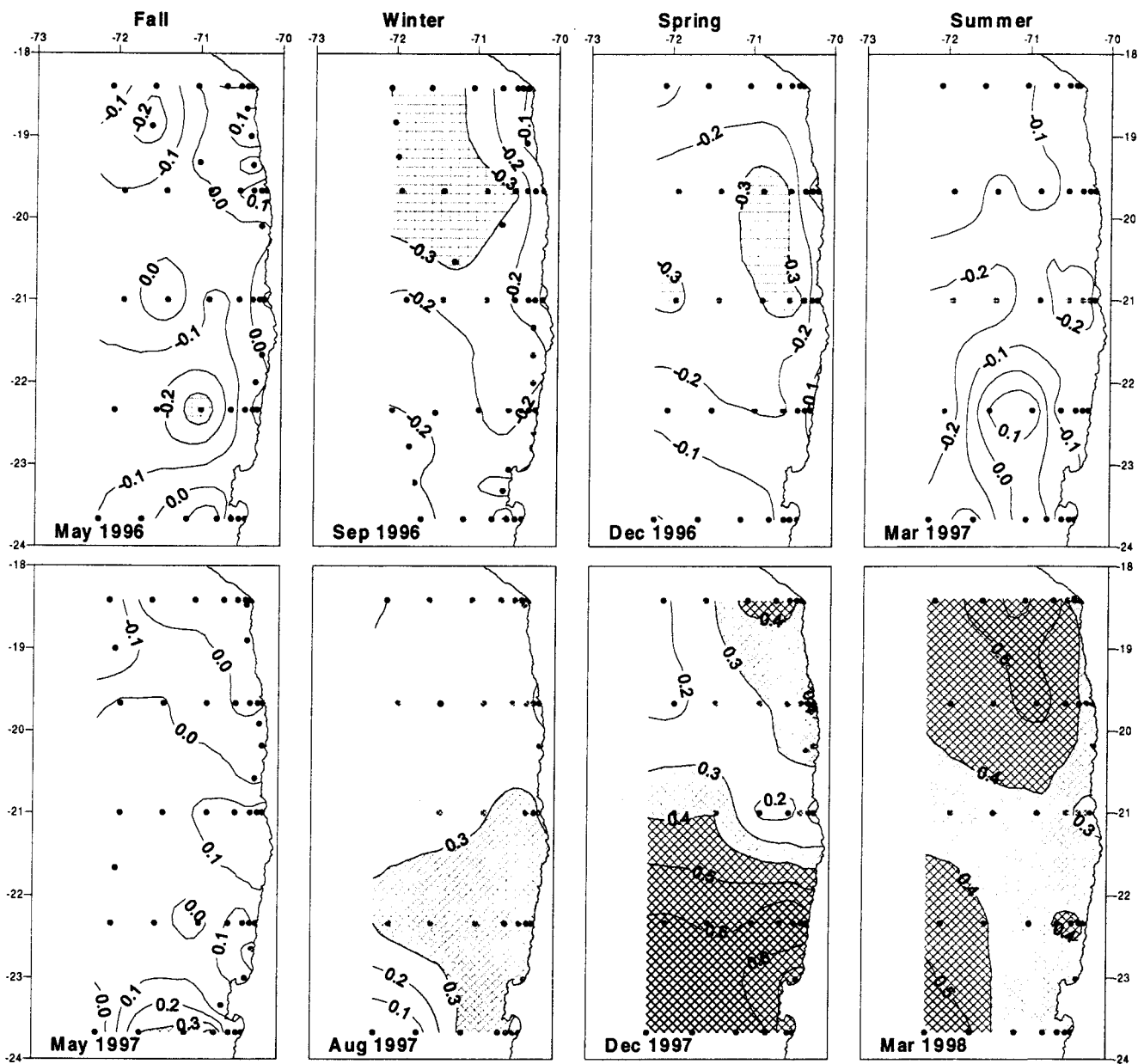


Fig. 5b

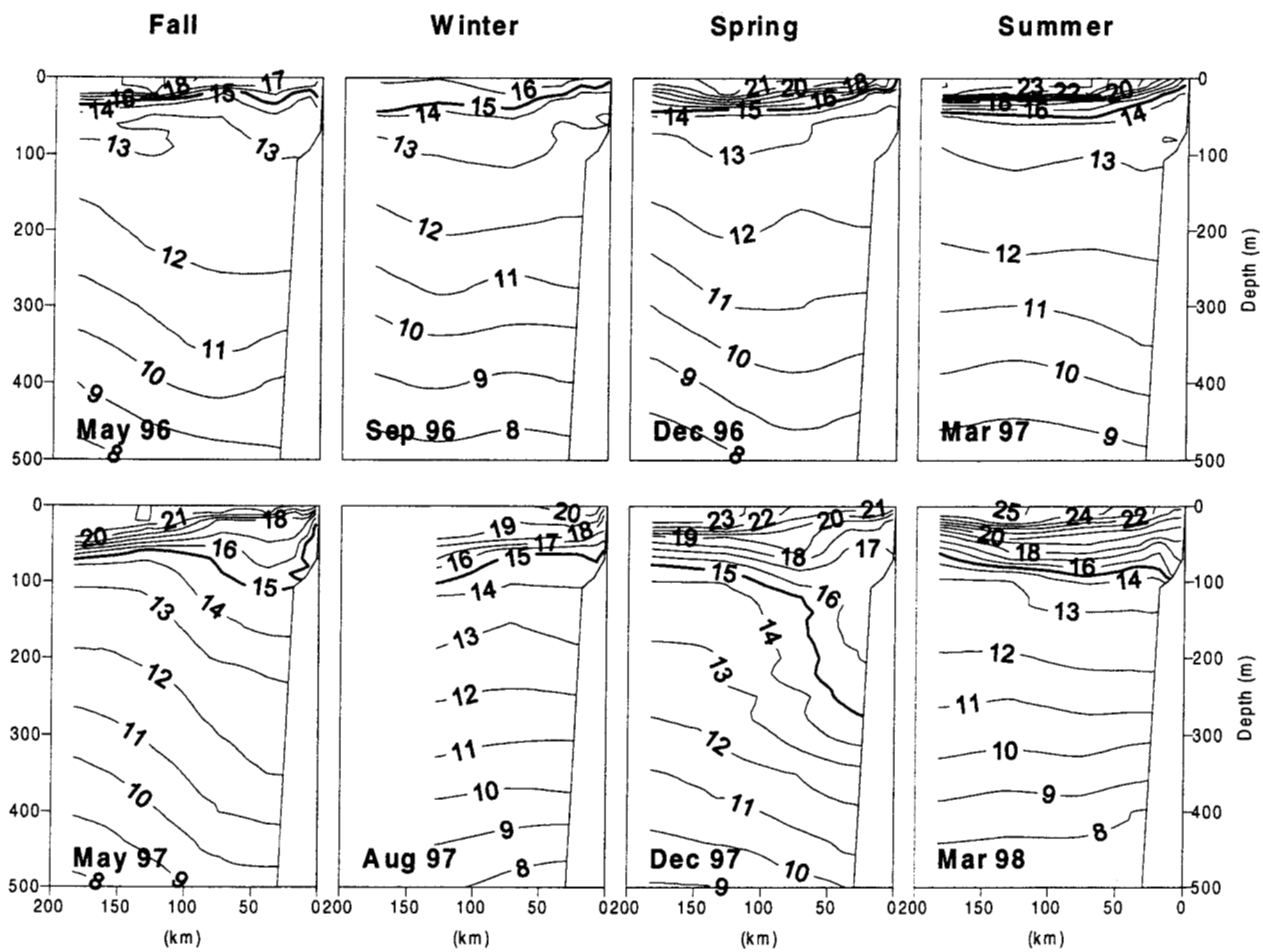


Fig. 6a

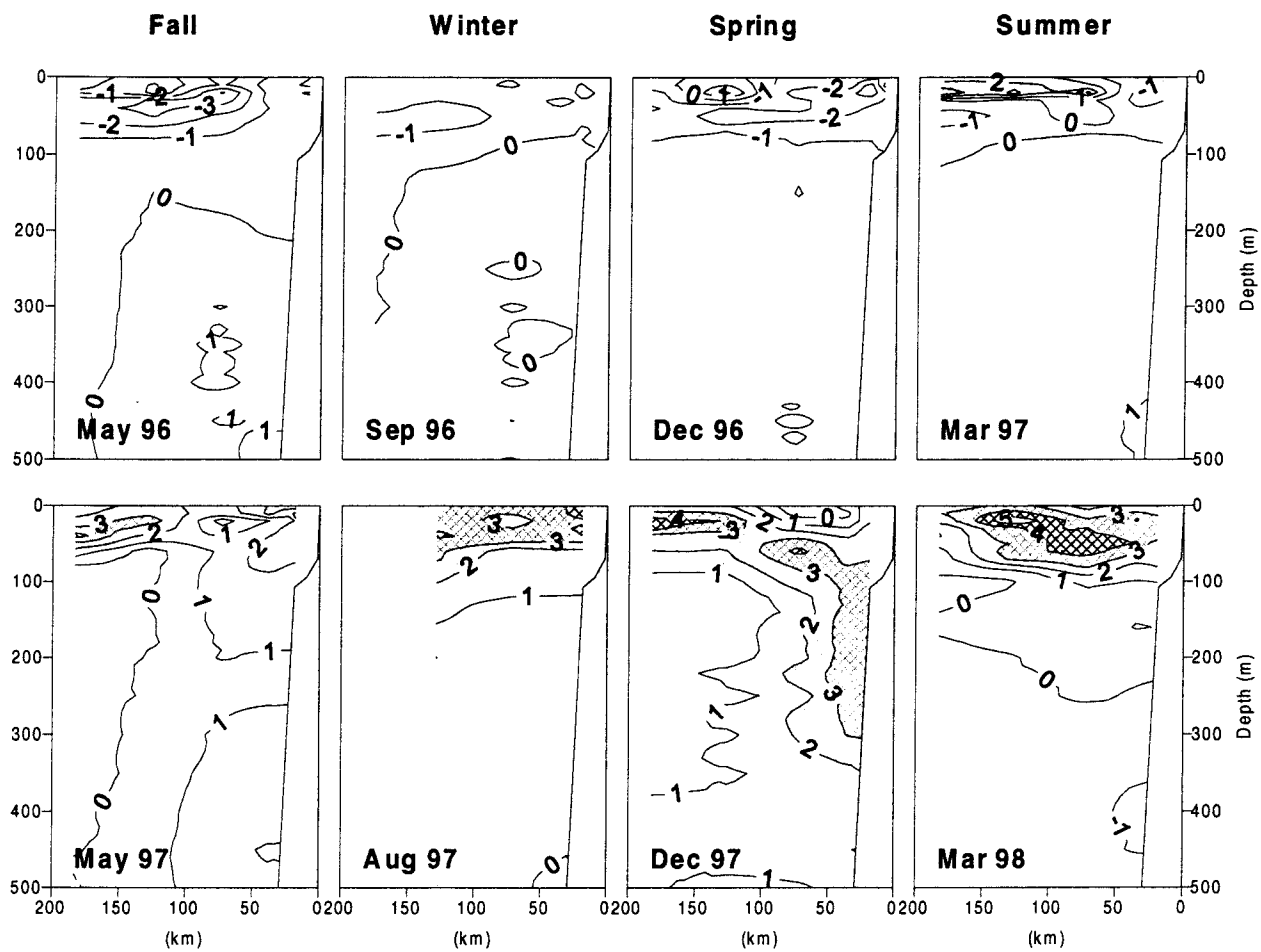


Fig. 6b

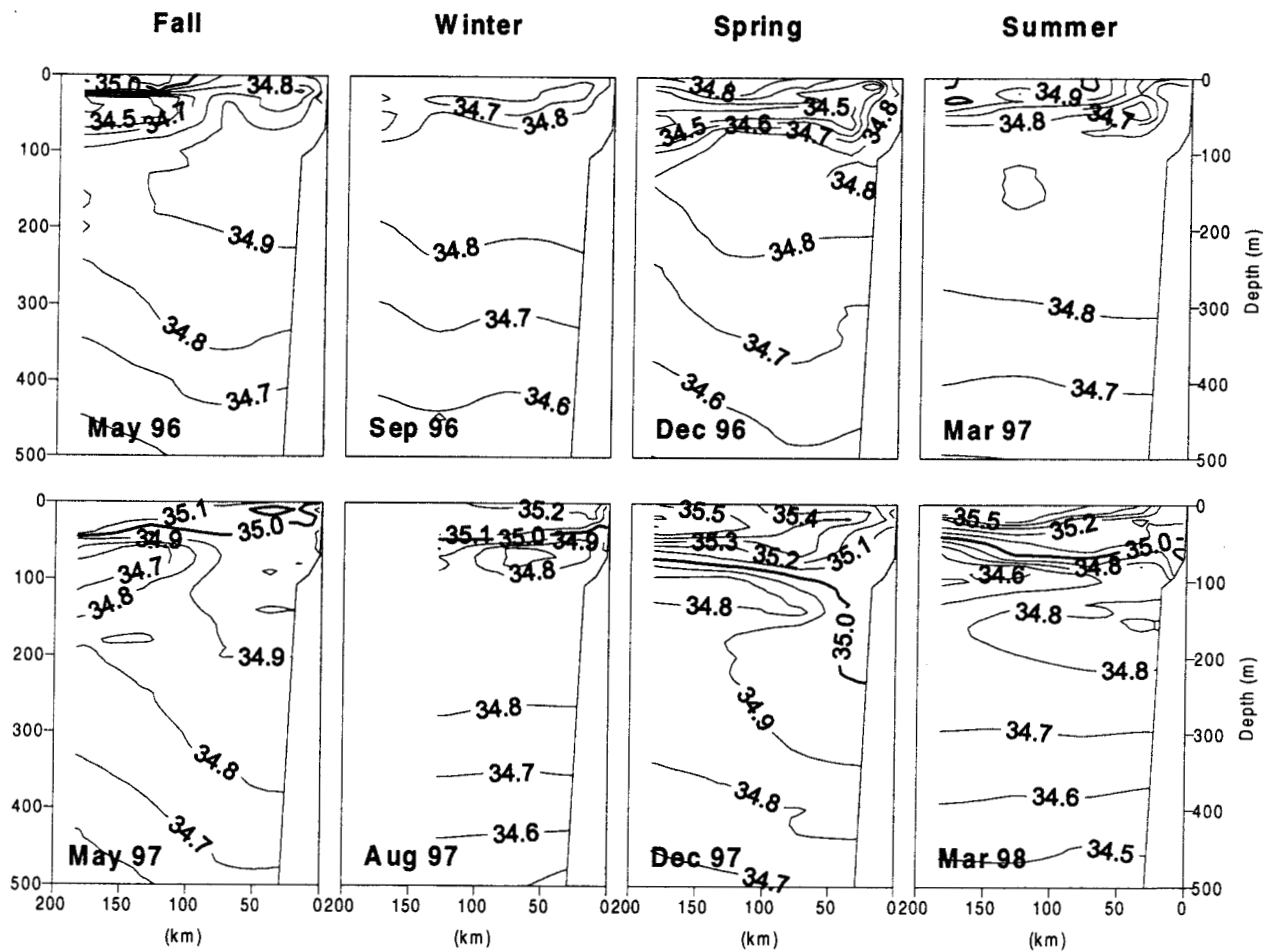


Fig. 7a

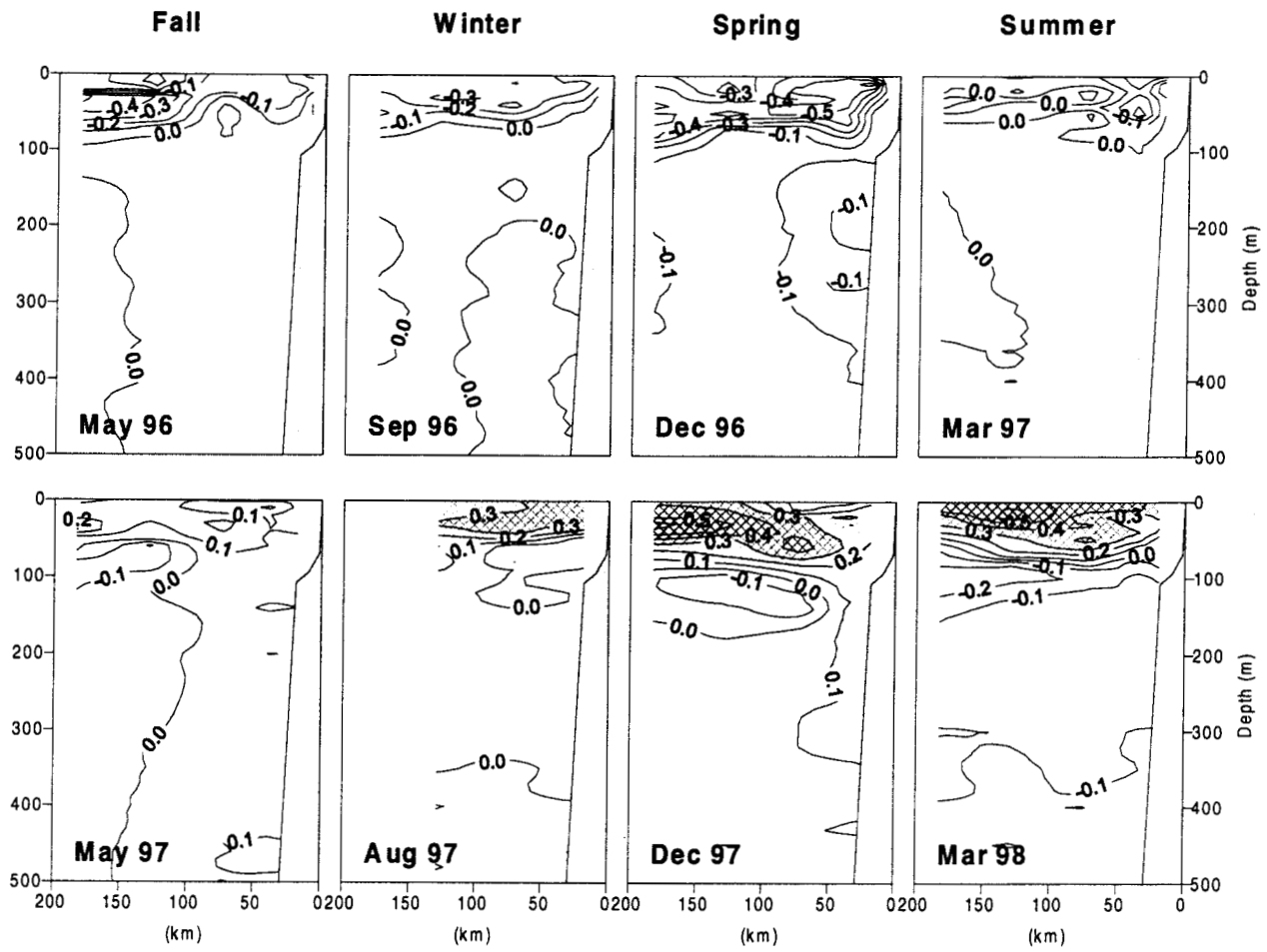


Fig. 7b



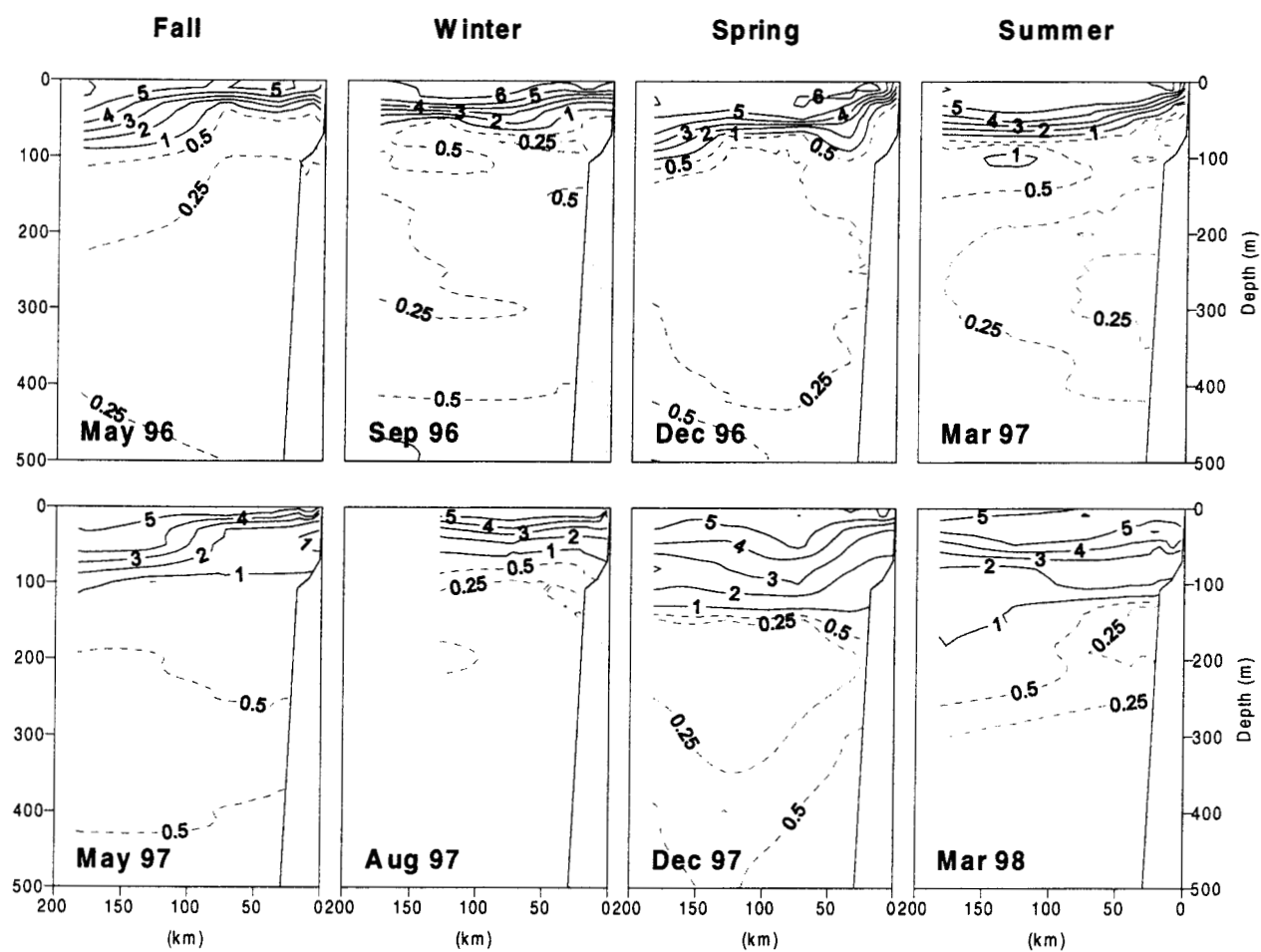


Fig. 8

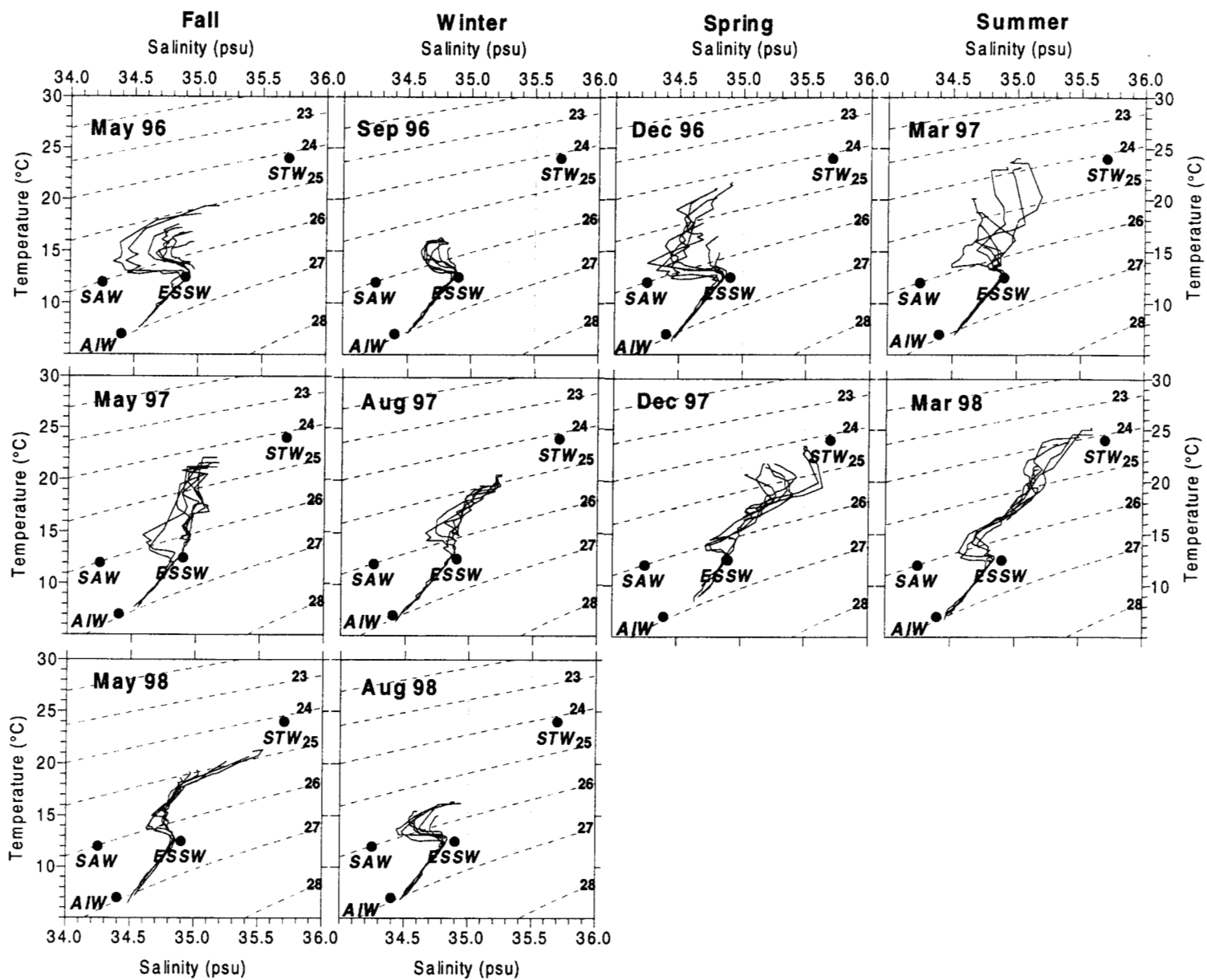


Fig. 9

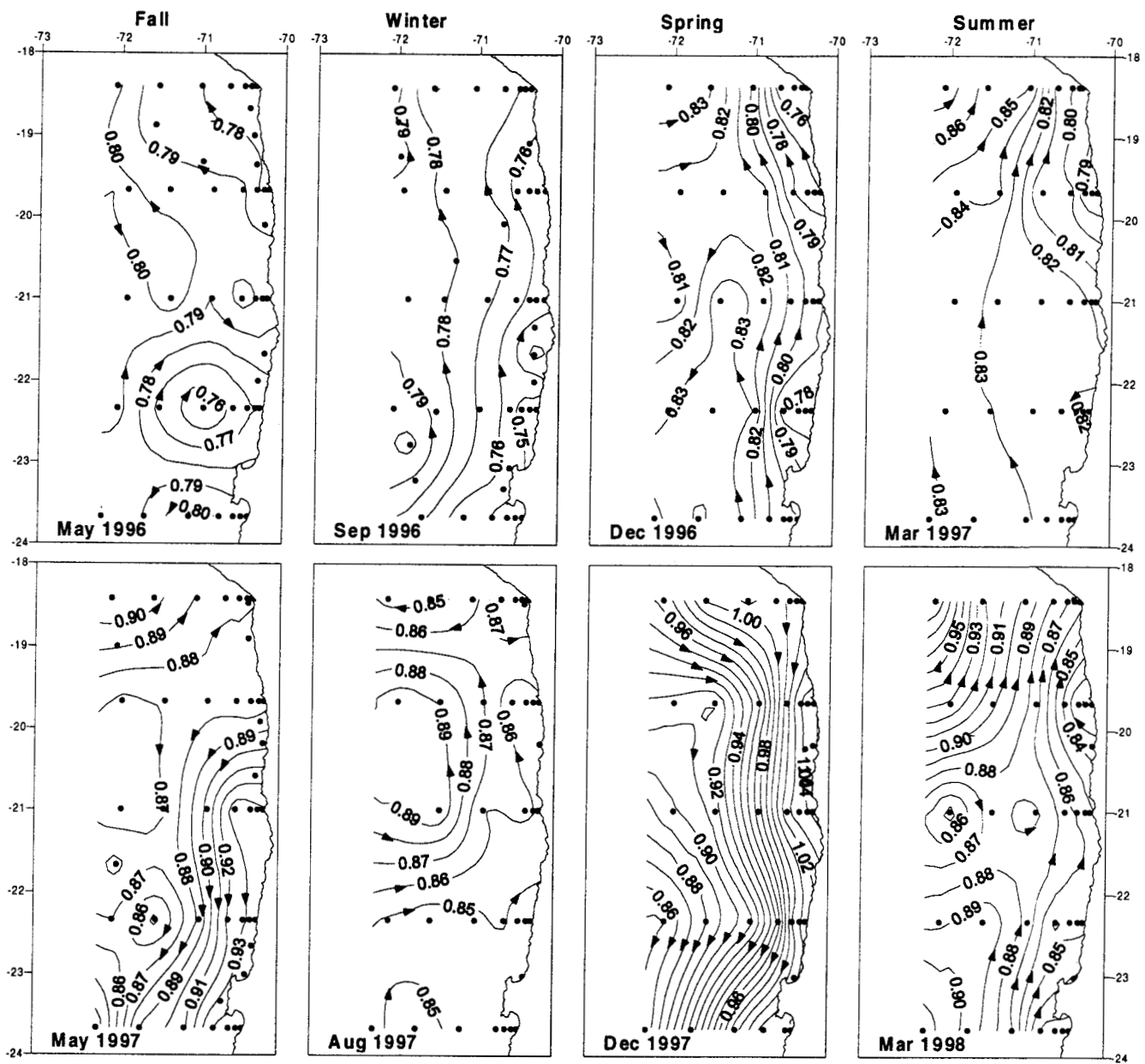


Fig. 10a

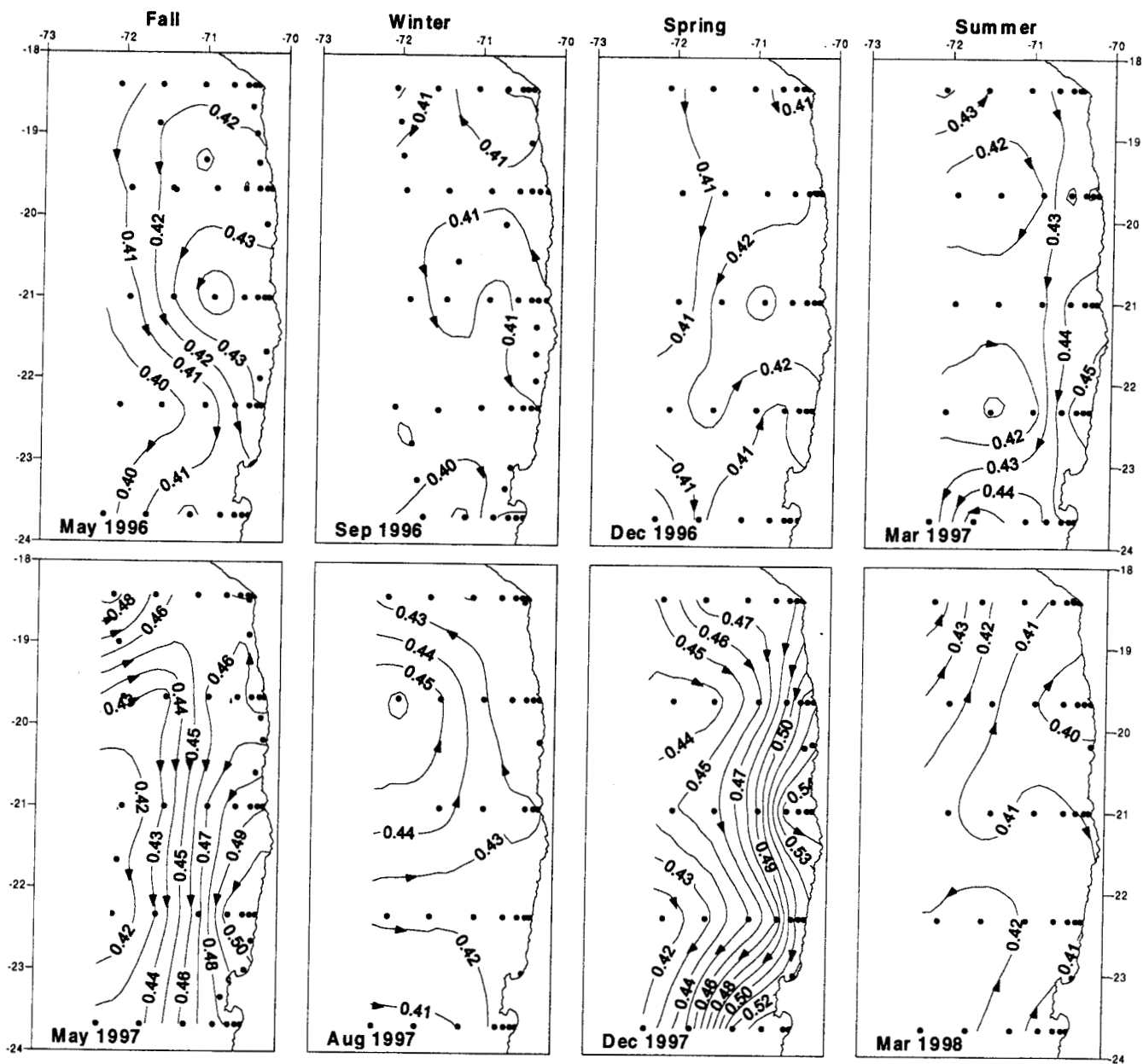


Fig. 1ob

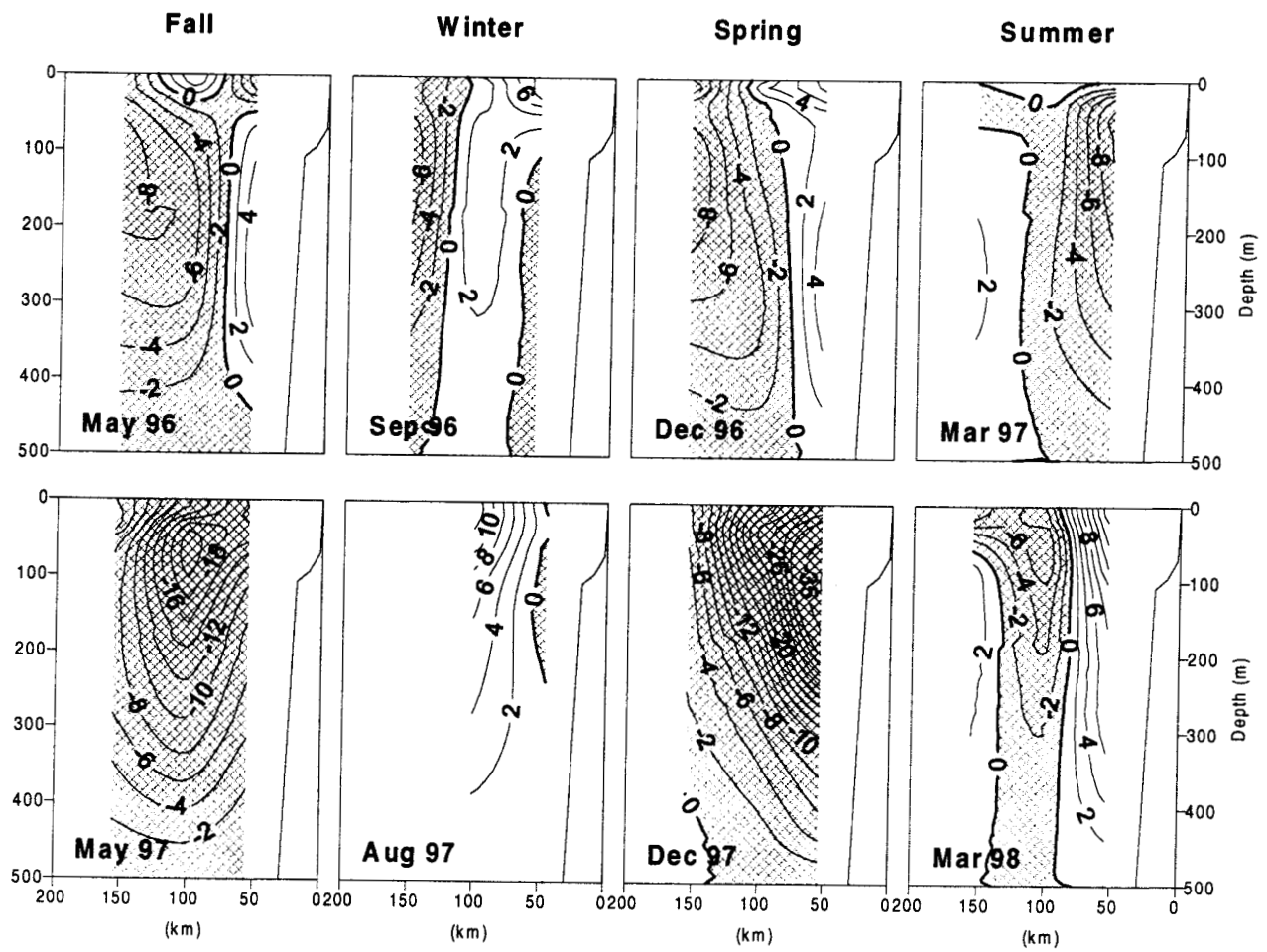


Fig. 11

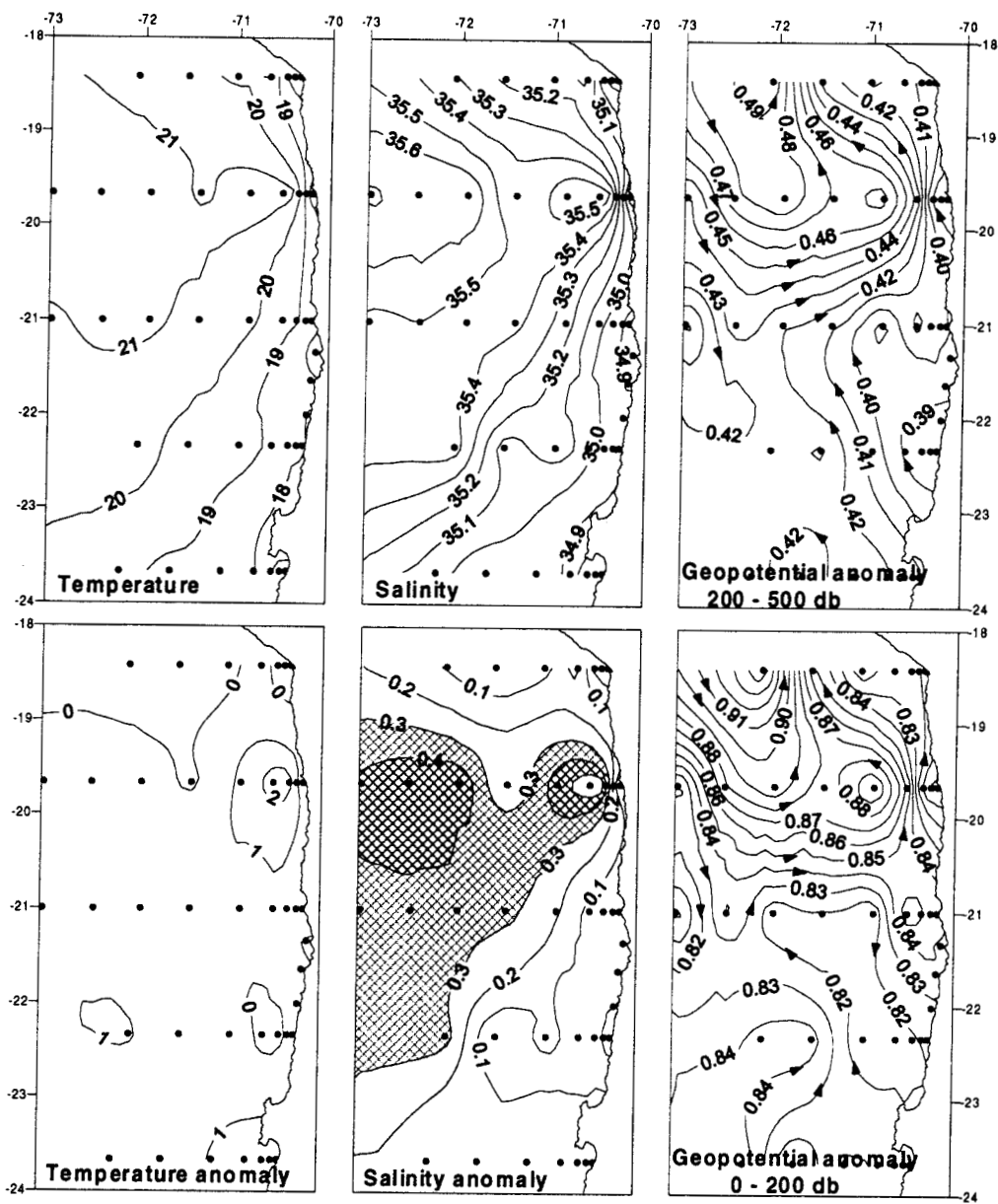


Fig. 12

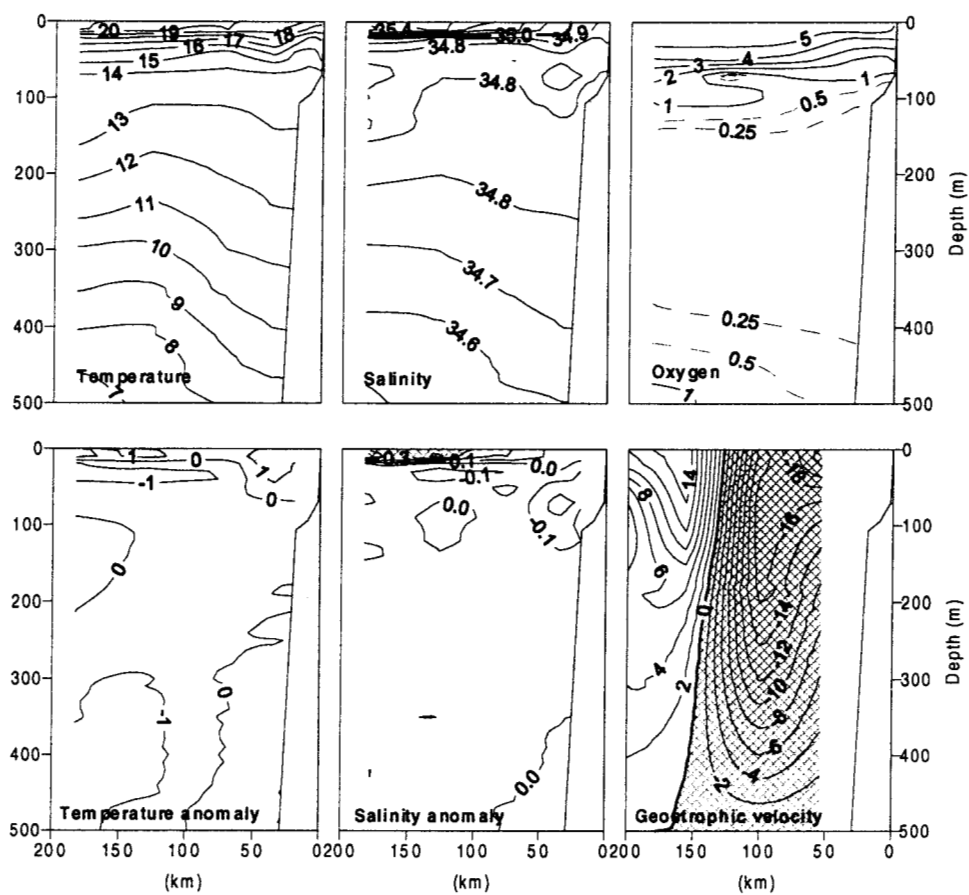


Fig. 13